Report No. NA-69-37
(RD-69-46)

INTERIM REPORT

Project No. 430-002-02X

EFFECT OF GROUND CRASH FIRE ON AIRCRAFT FUSELAGE INTEGRITY

DECEMBER 1969

DEPARTMENT OF TRANSPORTATION
FEDERAL AVIATION ADMINISTRATION
National Aviation Facilities Experimental Center
Atlantic City, New Jersey 08405

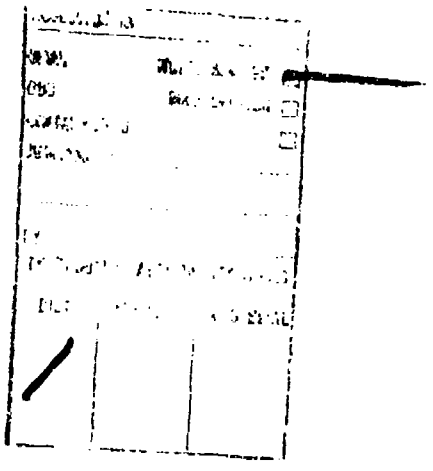

The Federal Aviation Administration is responsible for the promotion, regulation and safety of civil aviation and for the development and operation of a common system of air navigation and air traffic control facilities which provides for the safe and efficient use of airspace by both civil and military aircraft.

The National Aviation Facilities Experimental Center maintains laboratories, facilities, skills and services to support FAA research, development and implementation programs through analysis, experimentation and evaluation of aviation concepts, procedures, systems and equipment.

Copies of this report may be purchased for $3.00 each from the Clearinghouse for Federal Scientific and Technical Information (CFSTI), Springfield, Virginia, 22151.

1 STOCK LOCATION

2 DATE RECEIVED YR 70 MO 11 DAY 19

3 RECEIPT TYPE & FORMAT
☐ LOAN ☒ PC ☐ 35 MM ☐ CARDS ☐ MAGNETIC TAPE
☒ RETAIN ☐ MF ☐ 16 MM ☐ OTHER →

4 STOCK RECEIVED FOR SALE PC 28 MF

5 LOAN DOCUMENT RETURNED
DUE
OUT

6 TRANSACTION
NEW ITEM ☒ | DUPE ☐ | SUPERSEDES ☐ | PRIOR NUMBER ☐

7

8 SERIES NUMBERS (X-REF) ☒→
(A) NA-69-37 (B) FAA-RD-69-46

9 RELATED DOCUMENT ☐→

10 CONTRACTING OFFICE FAA

11 NOT FULLY LEGIBLE ☐ COLOR ☐

12 SCREEN ☐ REJECT
☐ OBTAIN BETTER COPY ☐ OUT OF PRINT SOD
☐ OBTAIN AUTHORITY ☐ ERRATA

13A ANNOUNCEMENT VOL 7 ISSUE 04 ☒ USG ☐ TAB ☐ UNANN

13B FAS ☐ YES ☒ NO

14 REPRODUCTION INSTRUCTIONS

BB → PRINT ↓	NO	1UP	2UP
NO	1	4	7
1UP	2	5	8
2UP	3	6	9
MIX	SAME SIZE	ORDER STOCK FROM	0

MAKE MICROFICHE ☒ YES ☐ NO ☐ ON DEMAND

15 PRESTOCK

	NO!	# COPIES
PC		
MF		A
PC DUE IN		

16 REMARKS

17 ACCESSION NUMBER AD 698 806

18 PAGES 75 | 19 SHEETS 2 | 20 LOW LIMIT PC MF | 21 ☐ SUBSCRIPTION

22 PRICES PC ☒ 3.00 MF ☒ 0.65 EXCEPTION PRICES

23 CATEGORY

24 DISTR CODE 1

25 INITIALS ACC JG A B C D

26 FILL FROM PAPER COPY ETC SS | MICRO-NEGATIVE sm

27 PUBLIC RELEASABILITY C

1/27 ap

1 ARCHIVES

Jan 14 20

FORM NBS 801 (7/69) • GPO 1968 – 315-288

U.S. DEPARTMENT OF COMMERCE
NATIONAL BUREAU OF STANDARDS
CLEARINGHOUSE FOR FEDERAL SCIENTIFIC AND TECHNICAL INFORMATION

DOCUMENT TRAVELER

EFFECT OF GROUND CRASH FIRE ON AIRCRAFT FUSELAGE INTEGRITY

Federal Aviation Administration
Atlantic City, New Jersey

December 1969

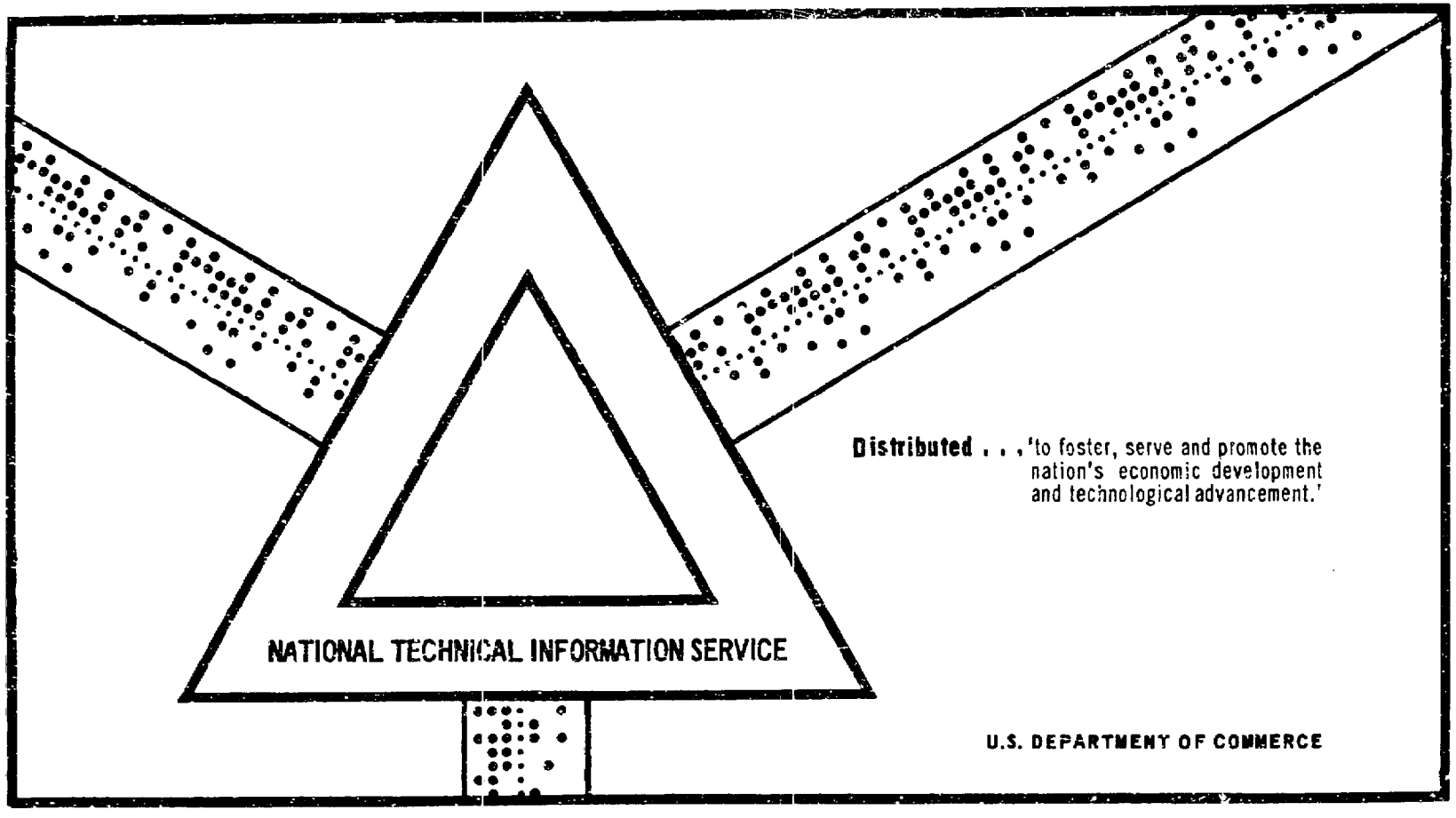

INTERIM REPORT

EFFECT OF GROUND CRASH FIRE ON AIRCRAFT FUSELAGE INTEGRITY

PROJECT NO. 430-002-02X

REPORT NO. NA-69-37
(RD-69-46)

Prepared by:
GEORGE B. GEYER

for

SYSTEMS RESEARCH AND DEVELOPMENT SERVICE

December 1969

DEPARTMENT OF TRANSPORTATION
Federal Aviation Administration
National Aviation Facilities Experimental Center
Atlantic City, New Jersey 08405

ABSTRACT

A mathematical model was formulated which permits a calculation to be made of the time required for damage to occur to the aluminum skin covering an aircraft fuselage when it is exposed to maximum spill fire conditions. The damage time was defined as the time required for the aluminum skin to melt.

The model was developed through consideration of the heat transfer rates by convection and radiation across a simplified aircraft fuselage configuration. The resulting differential equation was solved using a numerical technique. The results indicate that the minimum time required for skin damage to occur to the largest commercial aircraft now in service is less than 40 seconds. The fuselage damage time predictions, made through the use of the mathematical model, correspond closely with measurements made on simulated aircraft skin configurations employing a 40-foot, stainless-steel-covered section of a four-engine jet aircraft fuselage.

TABLE OF CONTENTS

LIST OF ILLUSTRATIONS

LIST OF ILLUSTRATIONS (continued)

INTRODUCTION

Purpose

The purpose of this investigation was to formulate a mathematical model which would permit a calculation to be made predicting the time required for an aluminum aircraft fuselage to melt when exposed to aircraft fuel fires of maximum severity, and also to obtain thermal data by conducting full-scale fire tests on a 40-foot, stainless-steel-covered fuselage section of a four-engine jet aircraft to verify the validity of the mathematical model for predicting fuselage fire damage time.

Background

The incidence of fire following survivable aircraft accidents frequently leads to tragic loss of life which could largely be prevented by a sufficiently rapid fire suppression response.

In incidents involving commercial aircraft, the large number of passengers aboard cannot be effectively evacuated through the fire by currently available techniques. However, as long as the aircraft fuselage retains its mechanical integrity following a survivable incident, the passengers are afforded some degree of protection from high temperatures, limited oxygen supply, and the toxic pyrolysis products of the cabin appointments.

Commercial airliners are constructed of the thinnest aluminum alloys consistant with structural requirements to effect the greatest economy in weight. These alloys melt at temperatures significantly lower than those of the flames from burning hydrocarbon fuels. Therefore, passengers may be exposed to maximum hazard conditions relatively soon after the incident occurs.

Until the present time, there has been no method available to predict, in a precise manner, either the time available to effect adequate fire suppression and passenger rescue or the time available to the fire department to respond to an aircraft accident. Therefore, this study was undertaken to obtain sufficient data to permit a meaningful estimation of these critical time parameters to be made.

DISCUSSION

General

The development of a mathematical model was based upon the heat transfer to and from an aircraft fuselage when exposed to two different fire test environments. The first condition exposed a stainless-steel-covered fuselage section to narrow rectangular JP-4 fuel fires located

at different distances on the upwind side, while the second concerned the fire situation of maximum severity and danger to the passengers; namely, the case where a large fire is adjacent to the fuselage.

Tests on the Stainless-Steel-Covered Fuselage

Description of the Tests: The test article comprised a 40-foot section of a four-engine jet aircraft fuselage completely covered externally with a 0.5-inch-thick layer of ceramic fiber insulation and 0.031-inch, Type 304, stainless steel sheets bolted to the fuselage. This configuration was employed to protect the fuselage from destruction by fire during the test program.

The instrumentation of the test fuselage and the pool fire locations relative to the fuselage are presented pictorially in Figure 1 and schematically in Figure 2.

The stainless steel panels were numbered consecutively from 1 to 10 starting at the rear of the fuselage. All instrumentation was confined to the upwind side of Panel No. 6. The thermocouple wires penetrated the fuselage from within at Stations T_a, T_b, T_c, T_d, T_e, T_f, and T_g and were tack-welded to the outside surface of the steel skin. The four water-cooled, nitrogen-gas-purged radiometers were mounted flush with the stainless steel skin and adjacent to the thermocouples at Stations RA, RB, RC, and RD (Figure 2). One thermocouple at Station T_h was extended 30 inches horizontally from the center of the fuselage to measure the air/flame temperature (Figure 3).

The upper interior portion of the fuselage is shown in Figure 4. All instrumentation wiring was contained in an underground conduit system leading from the center of the fuselage to the instrumentation trailer as shown in Figure 5.

Still and motion pictures were taken of each fire test for time data analysis and documentation from positions shown schematically in Figure 5.

The fire environment comprised three rectangular pits, 10 feet wide and 30 feet long, located equidistant from the ends and parallel to the fuselage. Each pit contained sufficient water to produce a level surface free from the intrusion of "islands" through the fuel surface. The JP-4 fuel charge to each pit was 0.35 gal/ft^2.

Four fire tests were performed in the following sequence: Test No. 1 in Pit A located 20 feet from the fuselage, Test No. 2 in Pit B located 10 feet from the fuselage, and Test No. 3 in Pit C which was adjacent to the fuselage. The fourth test was conducted employing

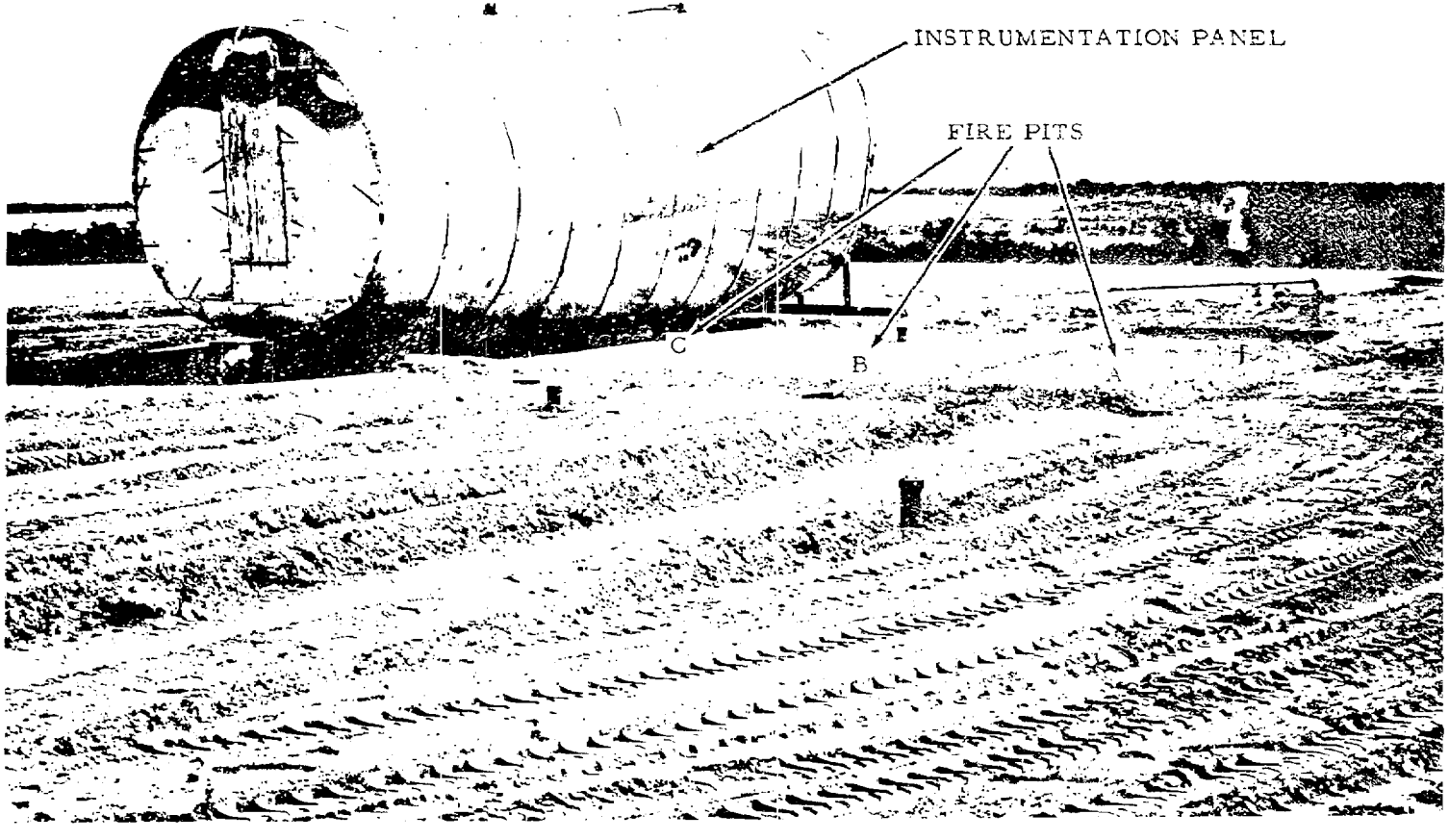

FIG. 1 EXTERIOR VIEW OF THE FUSELAGE SECTION AND THE FIRE PIT LOCATION

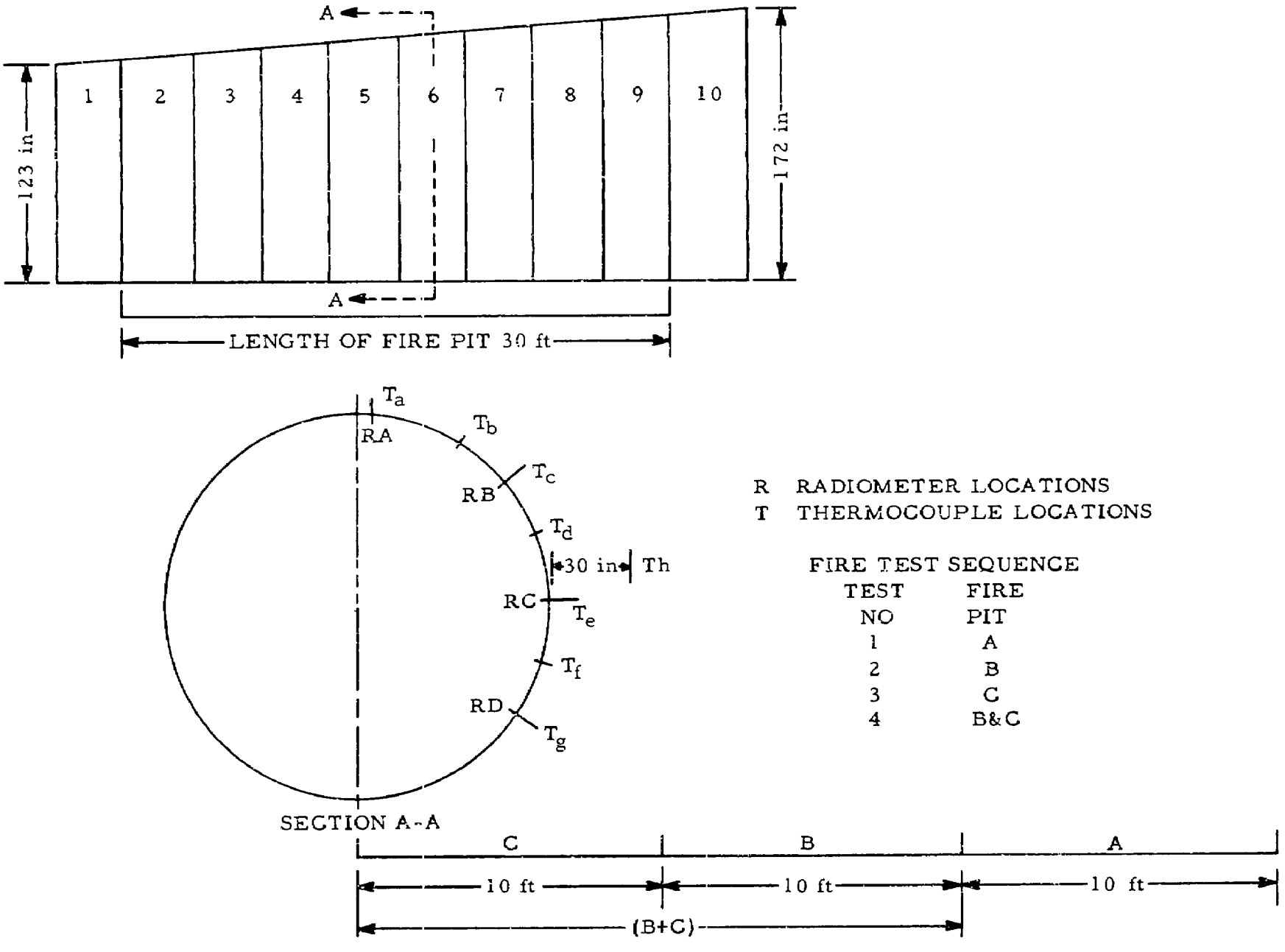

FIG. 2 SCHEMATIC DRAWING OF THE STAINLESS-STEEL-COVERED FUSELAGE AND LOCATION OF THE FIRE PITS (NOT TO SCALE)

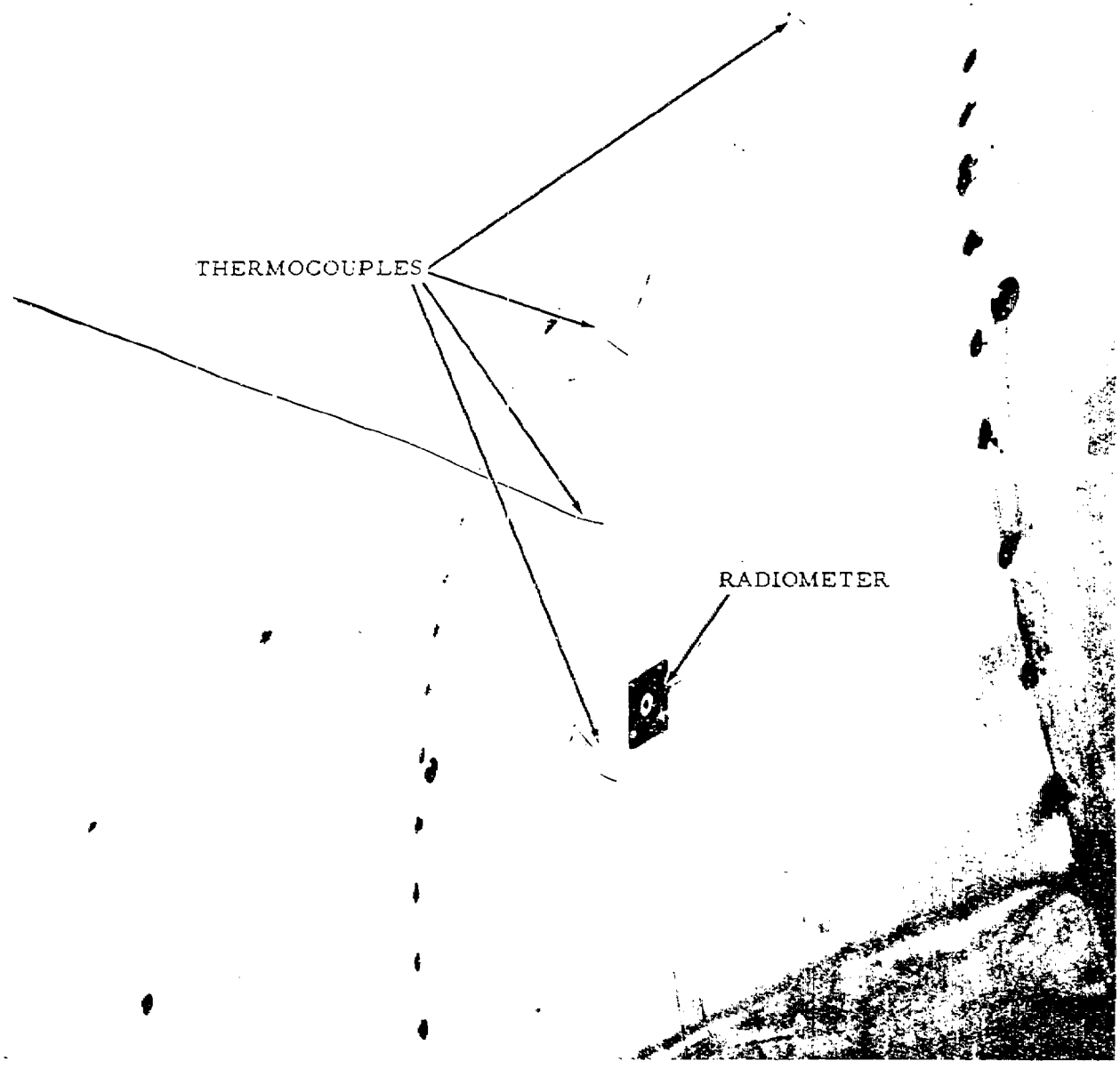

FIG. 3 CLOSEUP VIEW OF THE RADIOMETER AND THERMOCOUPLE INSTALLATIONS

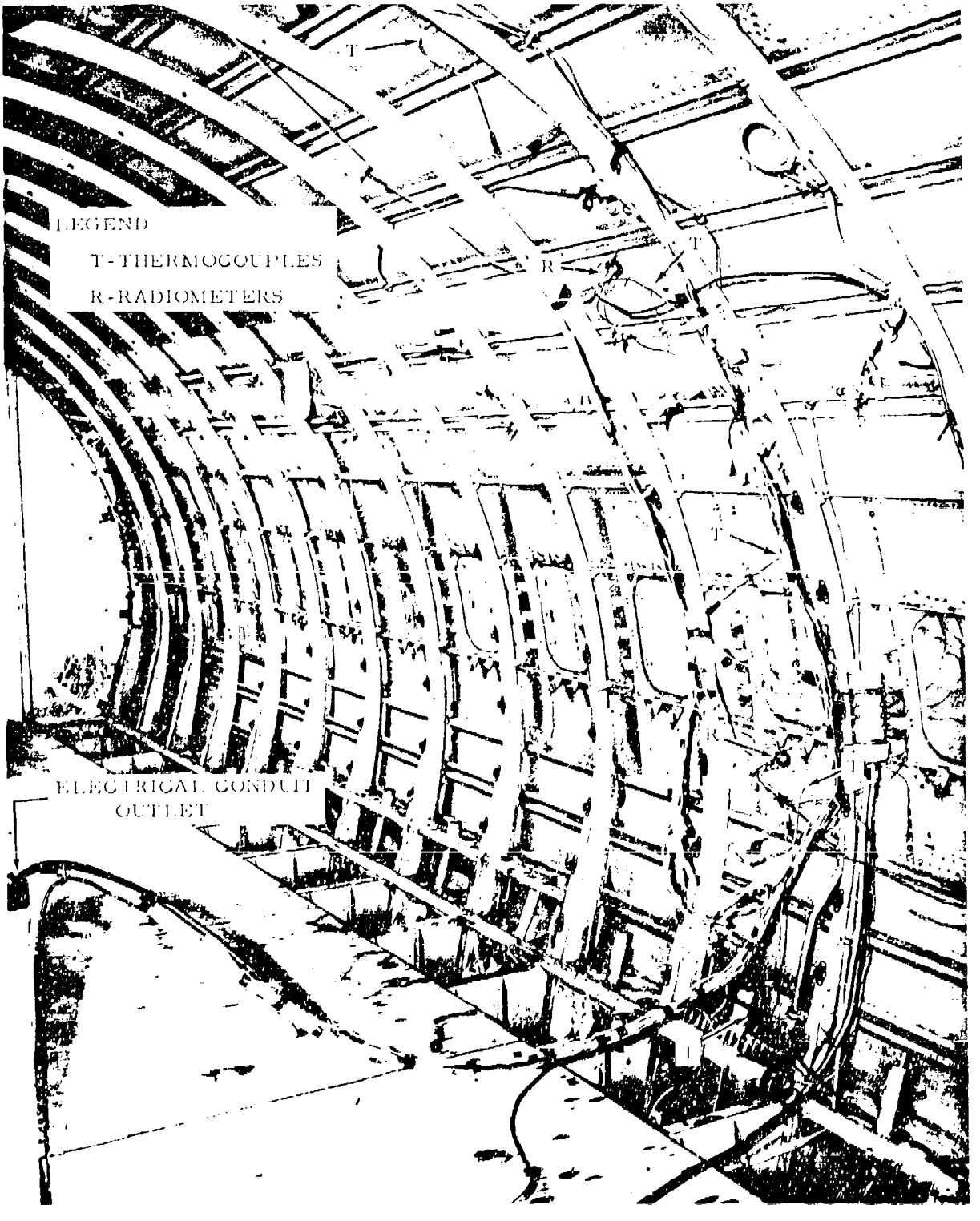

FIG. 4 INTERIOR VIEW OF THE FUSELAGE SHOWING THE THERMOCOUPLE AND RADIOMETER LOCATIONS

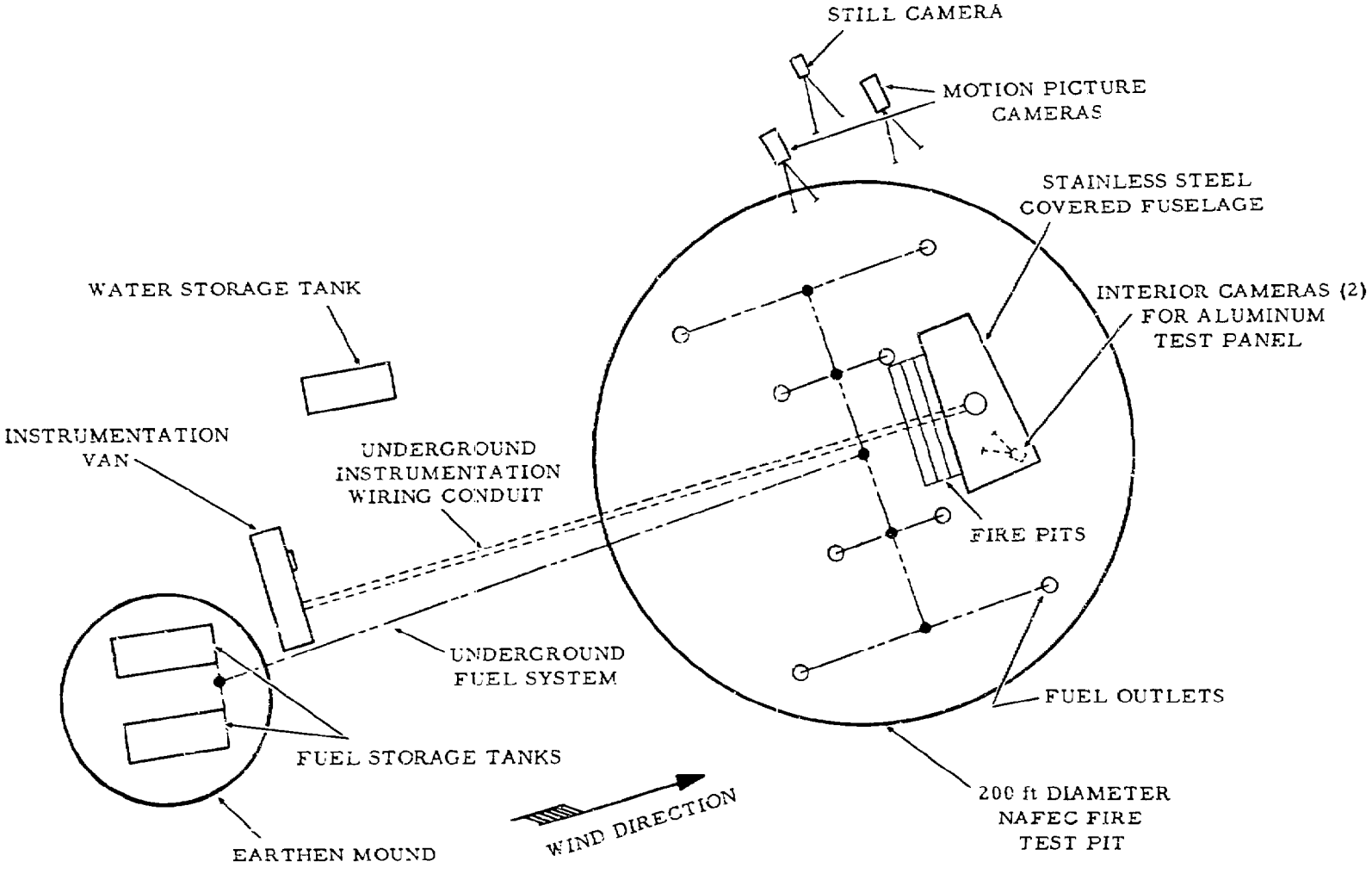

FIG. 5 PLAN VIEW OF THE FIRE TEST SITE (NOT TO SCALE)

Pits Nos. B and C simultaneously. This series of tests was designed to obtain thermal data concerning the effect of fire pit location on the exposed fuselage.

Results: The thermocouple and radiometer data obtained for the four stainless-steel-covered fuselage tests are presented in Appendix I. These data show that the most rapid rise in skin temperature was obtained in Test No. 2. Data from the other three tests showed a slower temperature rise in the aircraft skin which resulted from the different fire pit locations and the poor fire coverage caused by variable wind conditions on the relatively narrow fires at the time of the tests.

The stainless steel skin temperature rise for Test No. 2 is plotted as a function of time in Figure 6. An examination of the instrument data showed a delay of approximately 13 seconds from the time of ignition until the fire built up sufficiently to cover the instrumented area on the simulated aircraft fuselage. This time delay, due to fire buildup, was used to adjust the data points as shown by the solid points in Figure 6. Each solid point represents the same reading as the open point at the same temperature, but is has been shifted to the left side of the graph by 13 seconds. Therefore, the solid points are representative of an aircraft incident in which the fuselage is totally involved in fire with little or no delay in ignition time. This approach was consistent with the requirements for the development of a mathematical model which would predict the fuselage melting time representative of the immediate involvement of the fuselage in flames.

During the course of the stainless-steel-covered fuselage experiments, the effect of wind on free-burning pool fires (Reference 1) was evident and is considered to constitute an important factor in tactical aircraft firefighting techniques. The effect of wind is to bend the flame in the downwind direction, and the flame angle is a function of the wind velocity. The flame angle is defined as the angle of tilt of the flame from the vertical. The flame-trailing effect around the test article is shown for wind velocity of 6 to 8 mi/hr in Figure 7. In this test, the downwind edge of the fire pit was 20 feet from the centerline of the fuselage. Photographs (c) and (d) of Figure 7 show the large increase in the effective width of the fire caused by the flame-trailing phenomenon, and it will be noted that the flames are in actual contact with the fuselage. The temperature data presented in Appendix I, Test No. 1, Figure 1.5, show that the stainless steel skin temperature at Station T_d reached a maximum of 860°F in approximately 100 seconds after fuel ignition while the ambient air/flame temperature outside the fuselage rose to 1200°F in 30 seconds after fuel ignition.

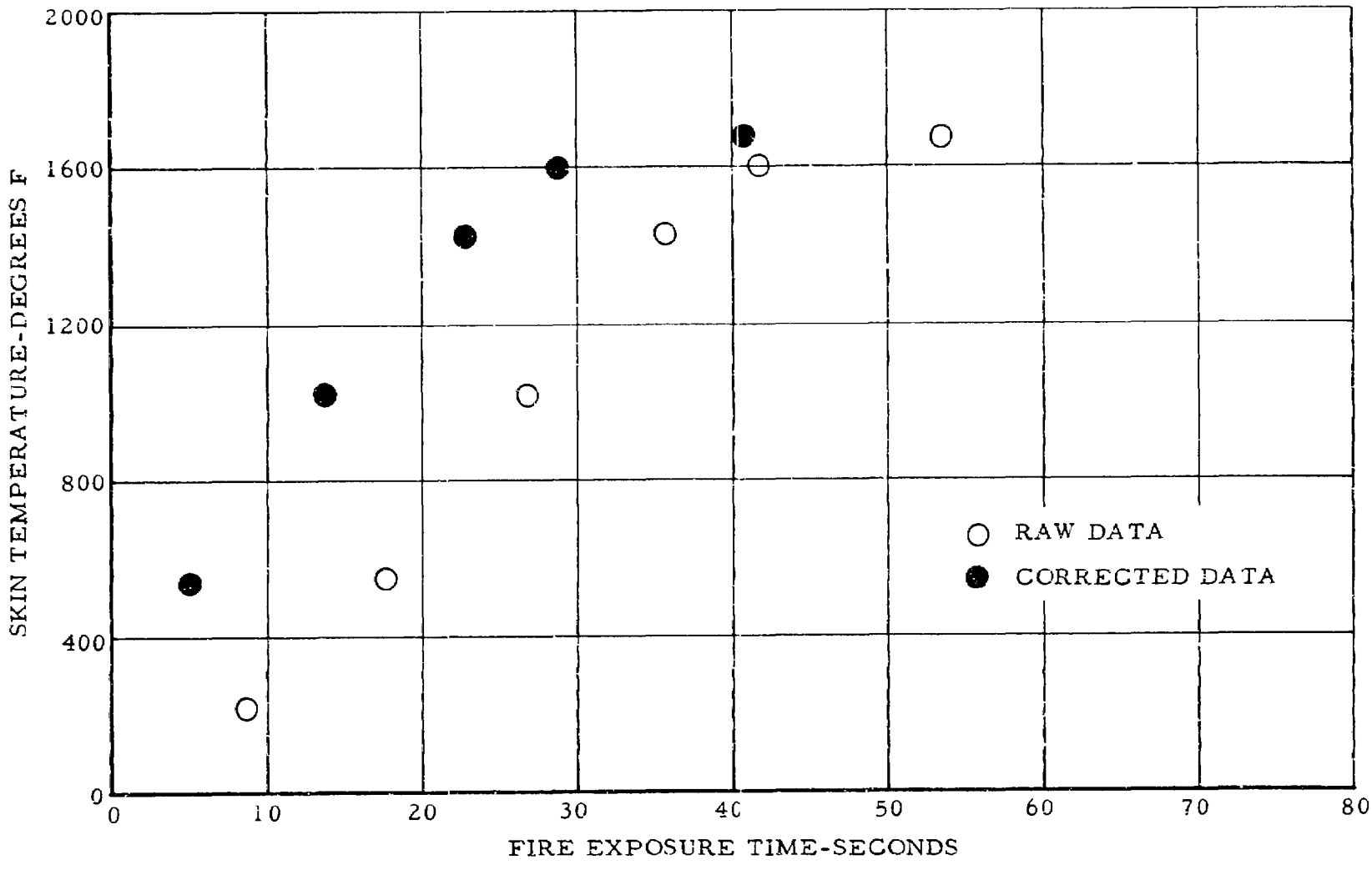

FIG. 6 SKIN TEMPERATURES FOR 0.031-INCH STAINLESS STEEL AS A FUNCTION OF FIRE EXPOSURE TIME

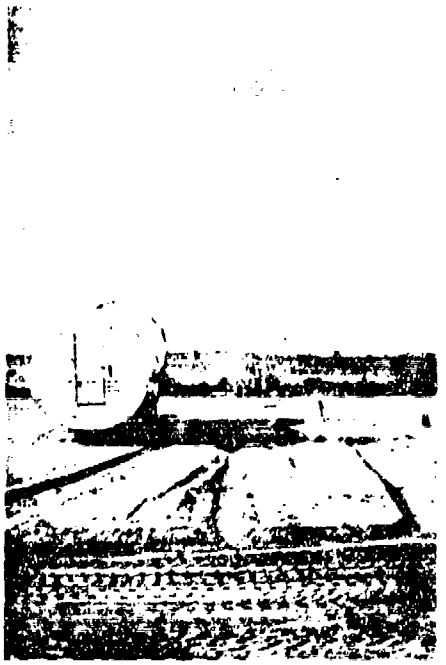

(a) Fire Pit Location

(b) Fuel Ignition

(c) Burning Time 10 Seconds

(d) Burning Time 30 Seconds

FIG. 7 EFFECT OF WIND ON POOL FIRES

Therefore, it is evident that relatively small fires remote and upwind from the fuselage may inflict serious fire damage to an aircraft fuselage as a result of the flame-trailing effect.

Tests on Aluminum Panels

Description of Tests: The second series of tests employed four different thicknesses of standard aluminum aircraft paneling inserted in three openings, 3 by 3 feet, cut through the fuselage and steel covering. Two of the four tests employed panels constructed of Alloy 2024-T3 conforming to Federal Specification QQ-A-362 (Alclad). One was 0.016 inch thick (Test No. 5), and the second was 0.040 inch thick (Test No. 6). The other two panels were constructed of Alloy 7075-T6 (Alclad) conforming to Federal Specification QQ-A-287 and were 0.020 inch thick (Test No. 7) and 0.090 inch thick (Test No. 8). Each panel was backed by a 2-inch-thick layer of "AA" fiberglas insulation with a density of 0.60 lb/ft^3 backed with a facing of polyvinylchloride. This configuration was designed to approximate standard aircraft construction and to provide all of the essential parameters necessary to verify the validity of the mathematical model. A cross-sectional drawing of the test panel construction is presented in Figure 8 and photographs of the instrumented panels in Figures 9 and 10. An exterior photograph of the fuselage section with panels installed for testing is shown in Figure 11.

The fire test environment for the aluminum panel tests utilized a 2500-ft^2 pit located on the upwind side and adjacent to the fuselage. The simulated spill consisted of 750 gallons of JP-4 fuel floated on water for leveling purposes. The large pit was designed to provide relatively complete fire envelopment of the fuselage and maximum fire exposure. Photographs of a typical fire test are contained in Appendix II, Figures 2.1, 2.2, 2.3, and 2.4.

The fuel was ignited from the instrument panel inside the instrument trailer by a high-intensity electric spark generated at the fuel surface and in the center of the upwind side of the pit as shown in Figure 12. After ignition, the fuel was allowed to burn until the skin temperature of any one of the panels reached 1200°F. The fire extinguishment operation was then started and continued until the fire was extinguished to prevent the destruction of the internal structure of the fuselage and instrumentation.

Inside the fuselage at the instant of fuel ignition, two electric clocks were activated which were located in the line of sight from the instrumentation camera to the aluminum test panels. One camera was positioned to photograph and record the burn-through time of the two upper panels and the second to cover the lower panel. These cameras are shown in Figures 9 and 10.

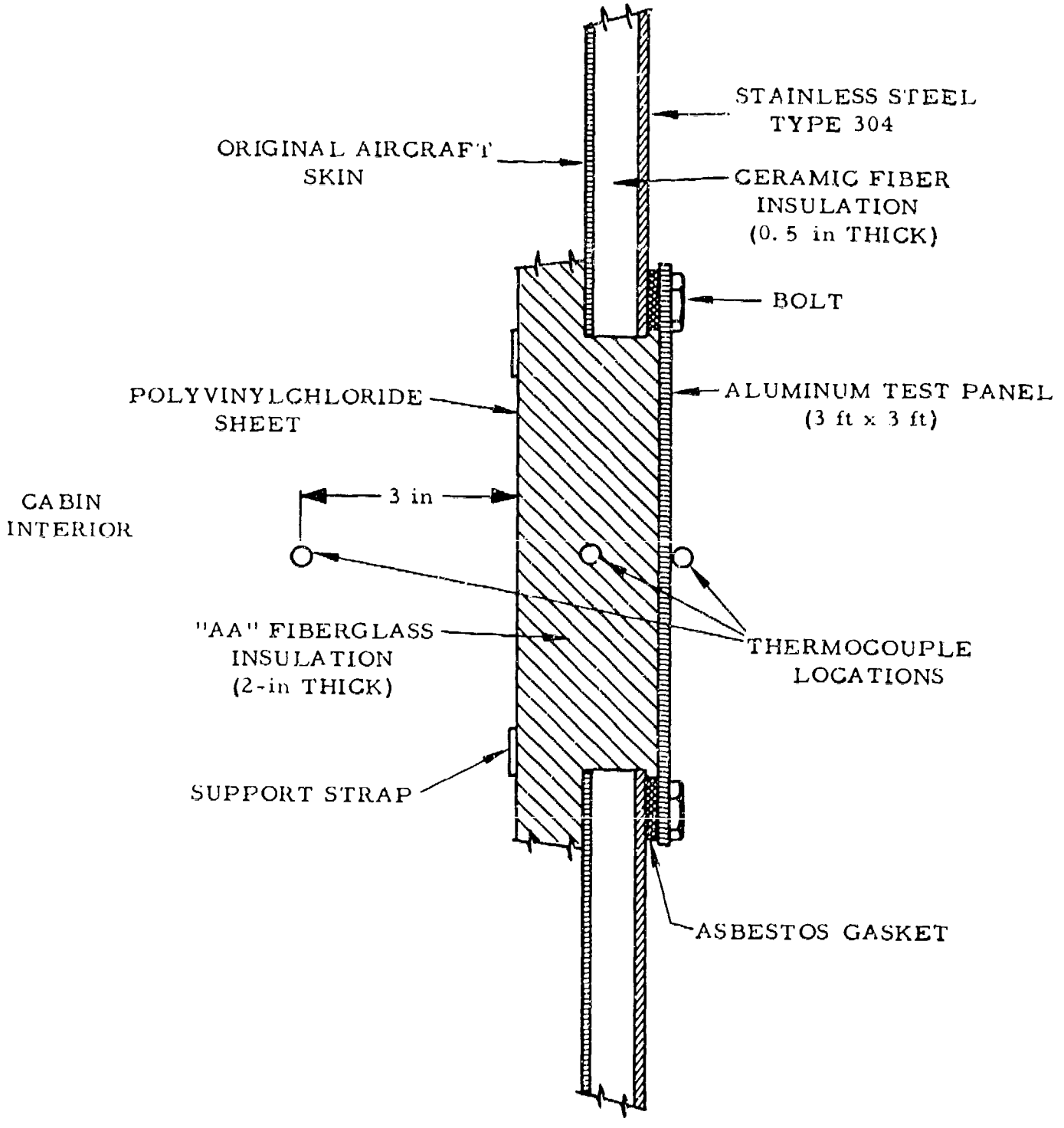

FIG. 8 CROSS SECTION OF THE ALUMINUM FIRE TEST PANEL CONFIGURATION
(NOT TO SCALE)

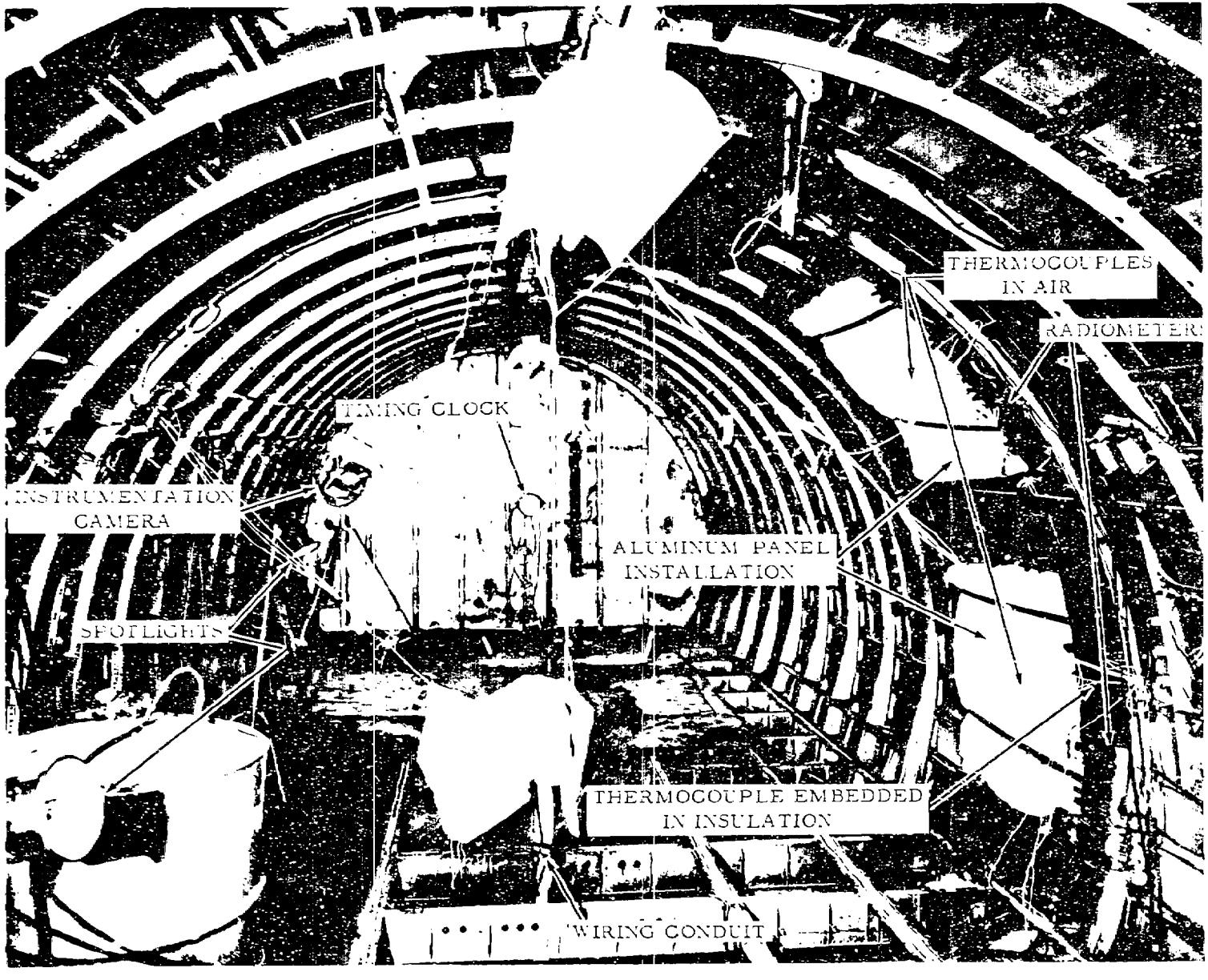

FIG. 9 UPPER ALUMINUM PANEL INSTALLATION

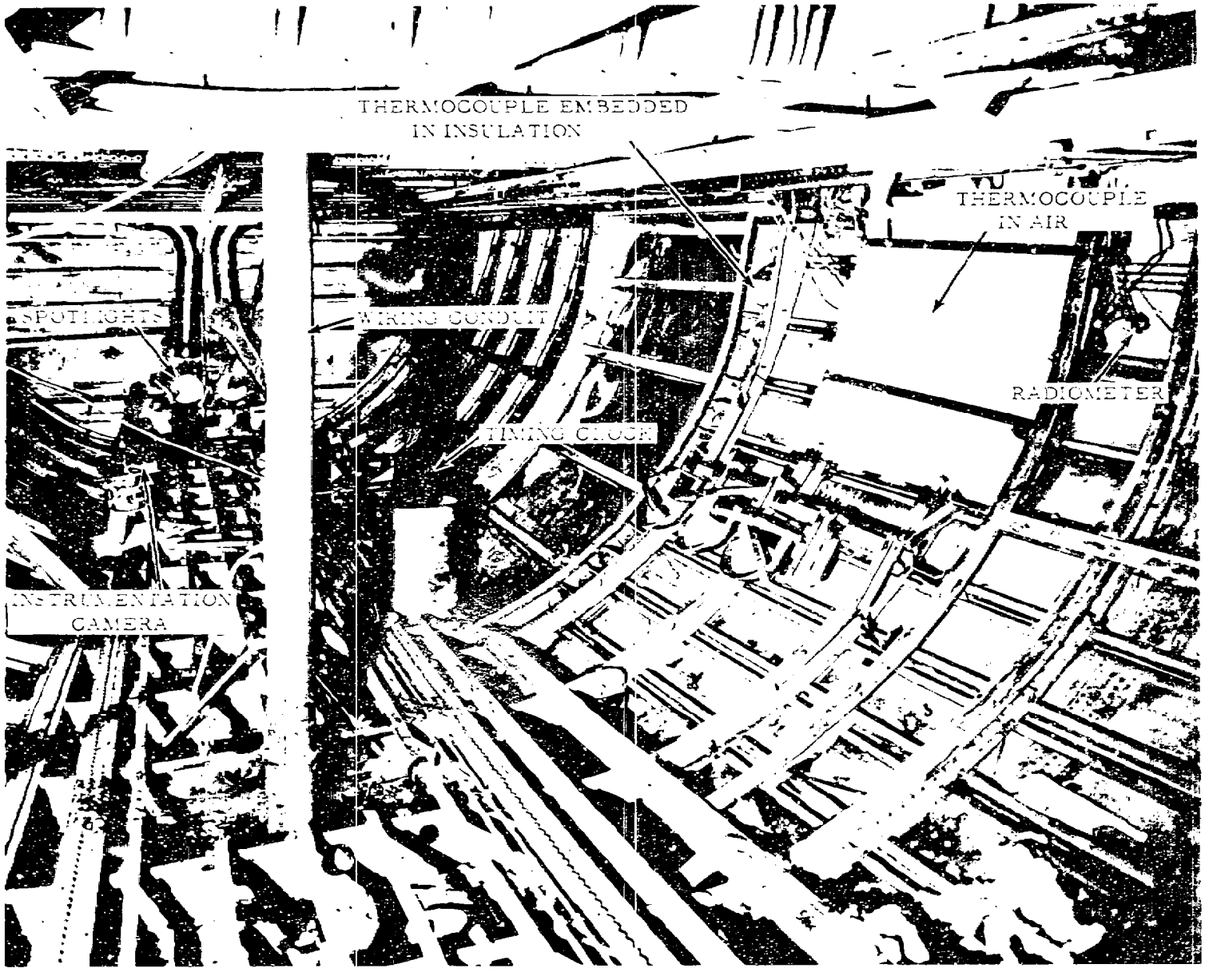

FIG. 10 LOWER ALUMINUM PANEL INSTALLATION

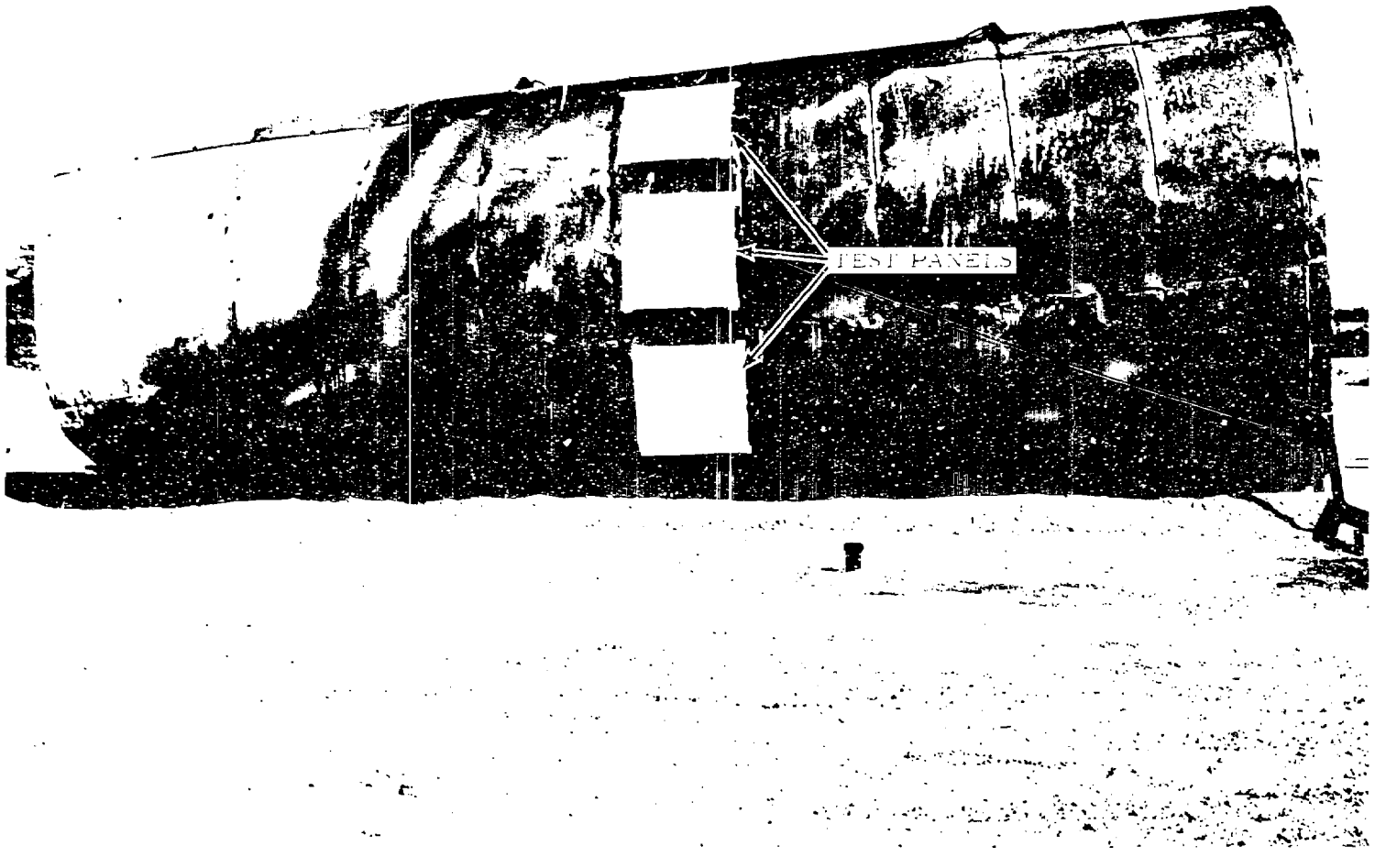

FIG. 11 EXTERIOR VIEW OF THE TEST PANELS IN POSITION

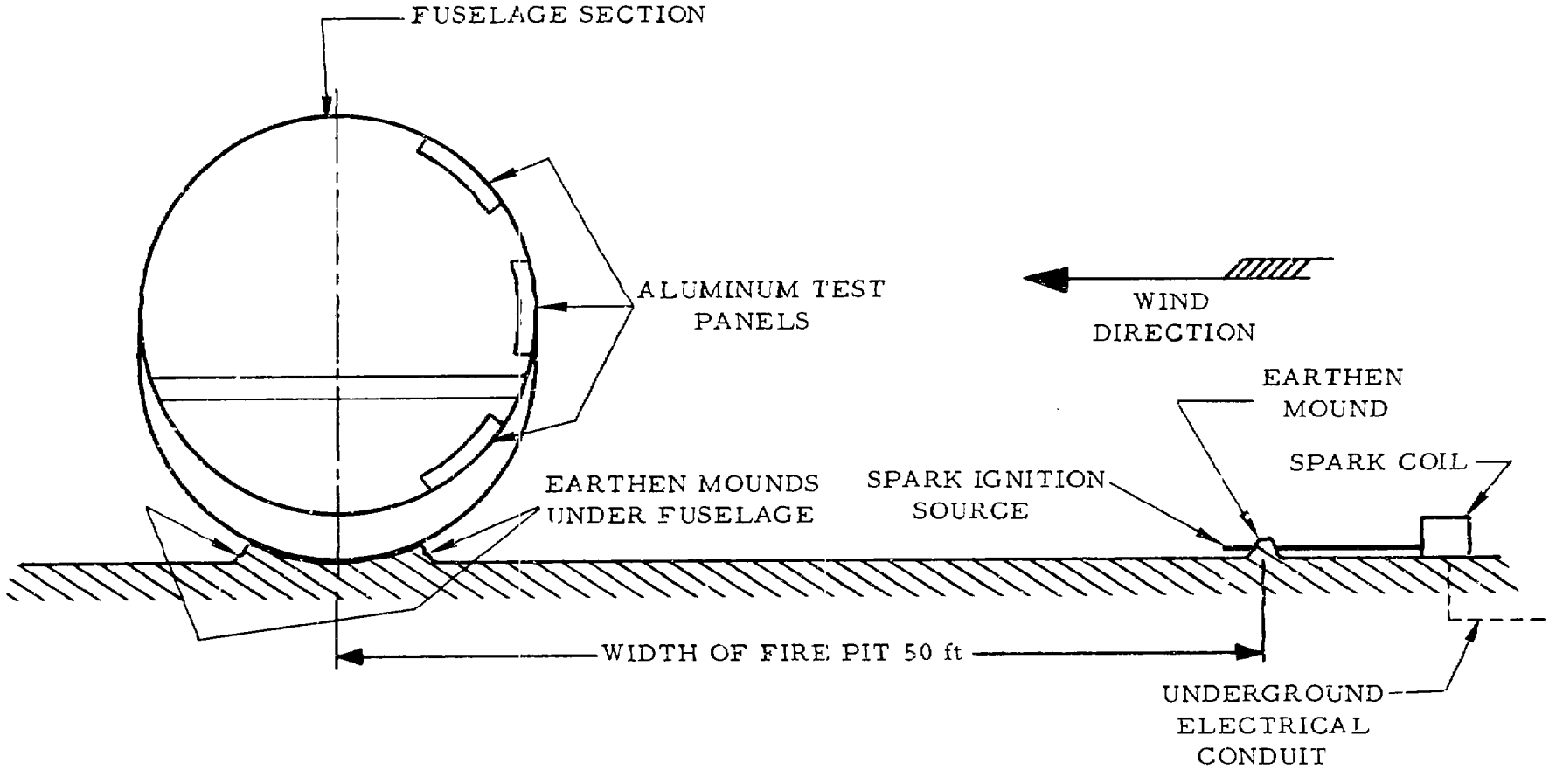

FIG. 12 ELEVATION VIEW OF THE FUSELAGE SECTION AND FIRE TEST PIT
(NOT TO SCALE)

Results: The results of the tests made on the simulated aluminum aircraft skins are presented in Figure 13 for a thickness of 0.020 inch and in Figure 14 for a thickness of 0.090 inch. In these graphs, the open points are the direct temperature measurements, and the solid points have been adjusted to allow for the flames to spread across the fire pit as described for the stainless steel tests. The radiometer and thermocouple data are presented in Appendix III and photographs representative of the fire conditions in Appendix II.

During the course of the fire tests involving the 0.016-inch, 0.020-inch, and 0.040-inch aluminum panels, it was observed that relatively large pieces of the test panels, as well as molten globules of metal, were ripped from the fuselage and carried from 50 to 60 feet downwind. Representative fragments of the panels and melted metal are shown in Figure 15. Some of the aluminum fragments showed severe heat crazing and embrittlement, although the edges displayed clean breaks and no melting was evident. Further observation of this phenomenon indicated that the thermal updraft around the fuselage probably reached 25 to 30 mi/hr which was apparently sufficient to rip off the thermally weakened metal before it could melt completely. However, only a few pieces of the 0.090-inch aluminum panels were retrieved on the downwind side of the fuselage, and the larger part of these panels was found completely fused under the fuselage.

Time-Temperature History of Aircraft Skin Heating

Development of a Mathematical Model: The development of a mathematical model predicting fuselage fire damage time (melting) was based upon the quantity of heat transferred to and from an aircraft fuselage during exposure to fire. Primary concern was given to conditions where the fire surrounds the aircraft and the flames impinge directly on the fuselage. This environment most closely approaches the steady-state conditions necessary for the mathematical treatment of a free-burning pool fire.

Figure 16 shows the simplified model of the aircraft skin backed by a layer of thermal insulation through which the heat balance was made. In the model, heat gain to the aircraft skin is assumed to be by radiation and convection from the fire, while heat loss is due to (1) radiation, (2) convection, and (3) conduction. The difference between the heat gain and heat loss is accumulated by the skin and causes a rise in its temperature. This relationship may be expressed in general terms as follows:

$$\text{Heat Accumulated} = \text{Heat Input} - \text{Heat Loss}$$

The detailed mathematical treatment of this thermal balance is presented in Appendix IV.

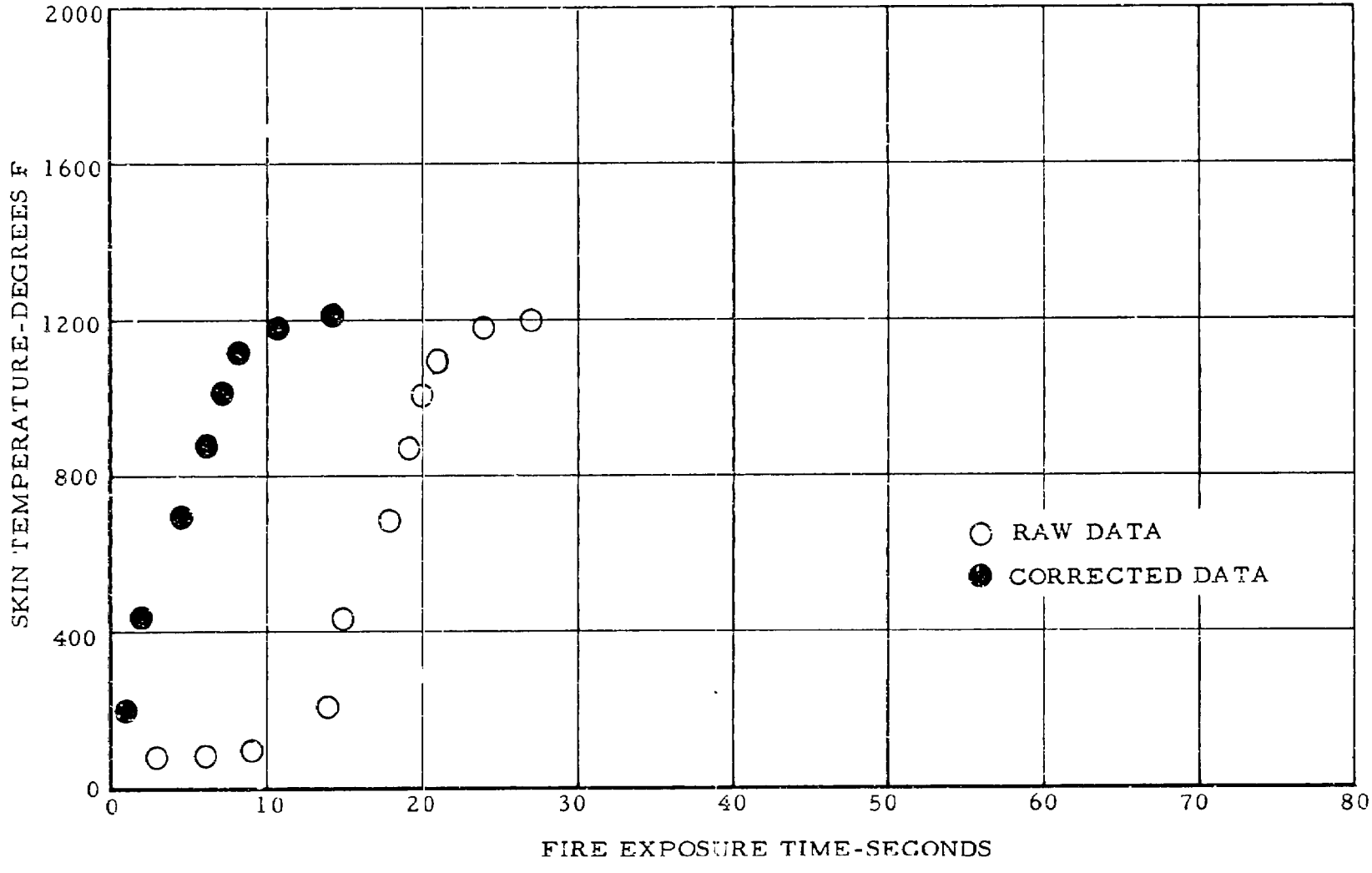

FIG. 13 EXPERIMENTAL SKIN TEMPERATURES FOR 0.020-INCH ALUMINUM AS A FUNCTION OF FIRE EXPOSURE TIME

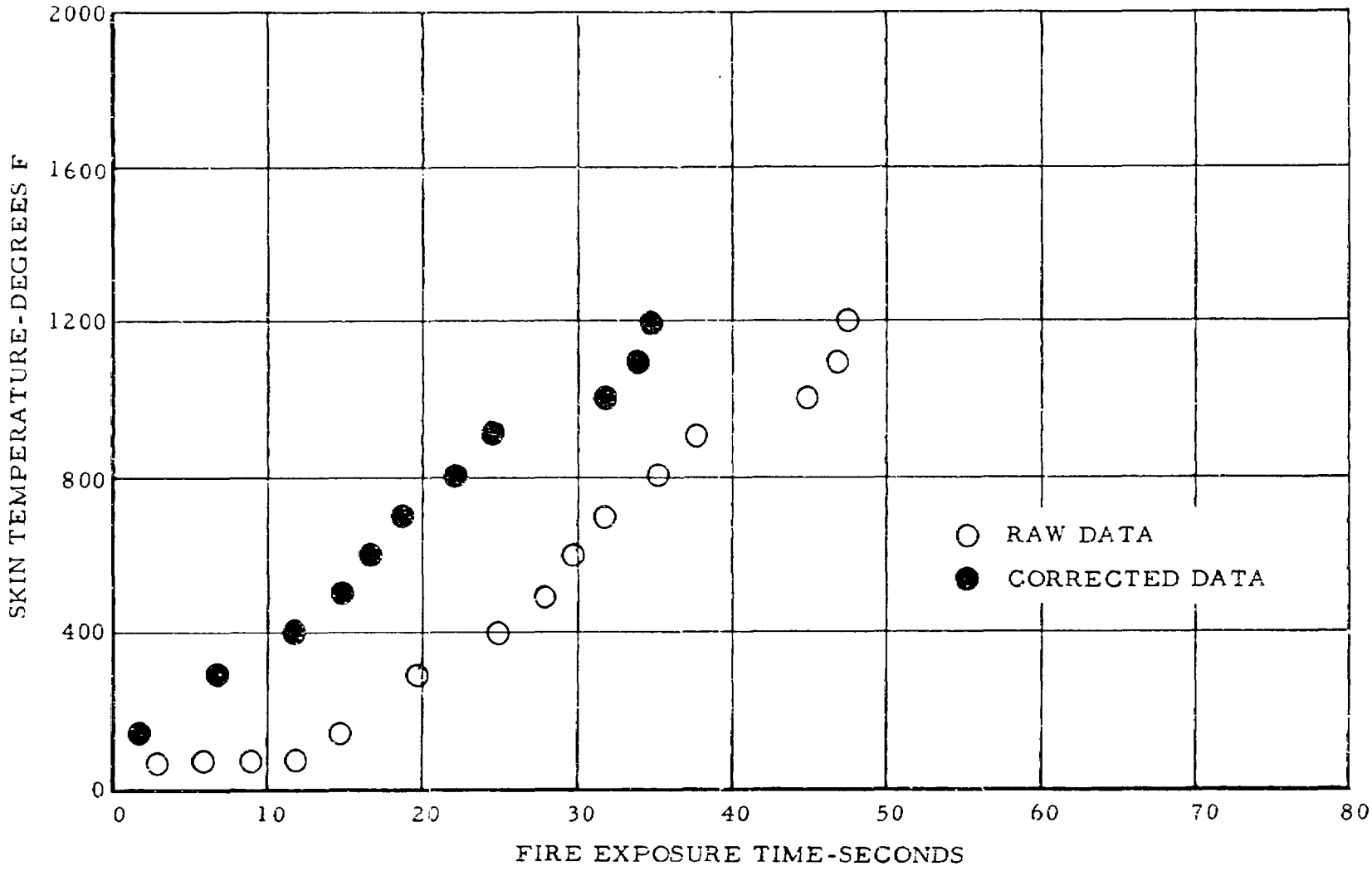

FIG. 14 EXPERIMENTAL SKIN TEMPERATUPES FOR 0.090-INCH ALUMINUM AS A FUNCTION OF FIRE EXPOSURE TIME

FIG. 15 FRAGMENTS OF ALUMINUM PANELS RETRIEVED 50 TO 60 FEET DOWNWIND FROM THE FUSELAGE

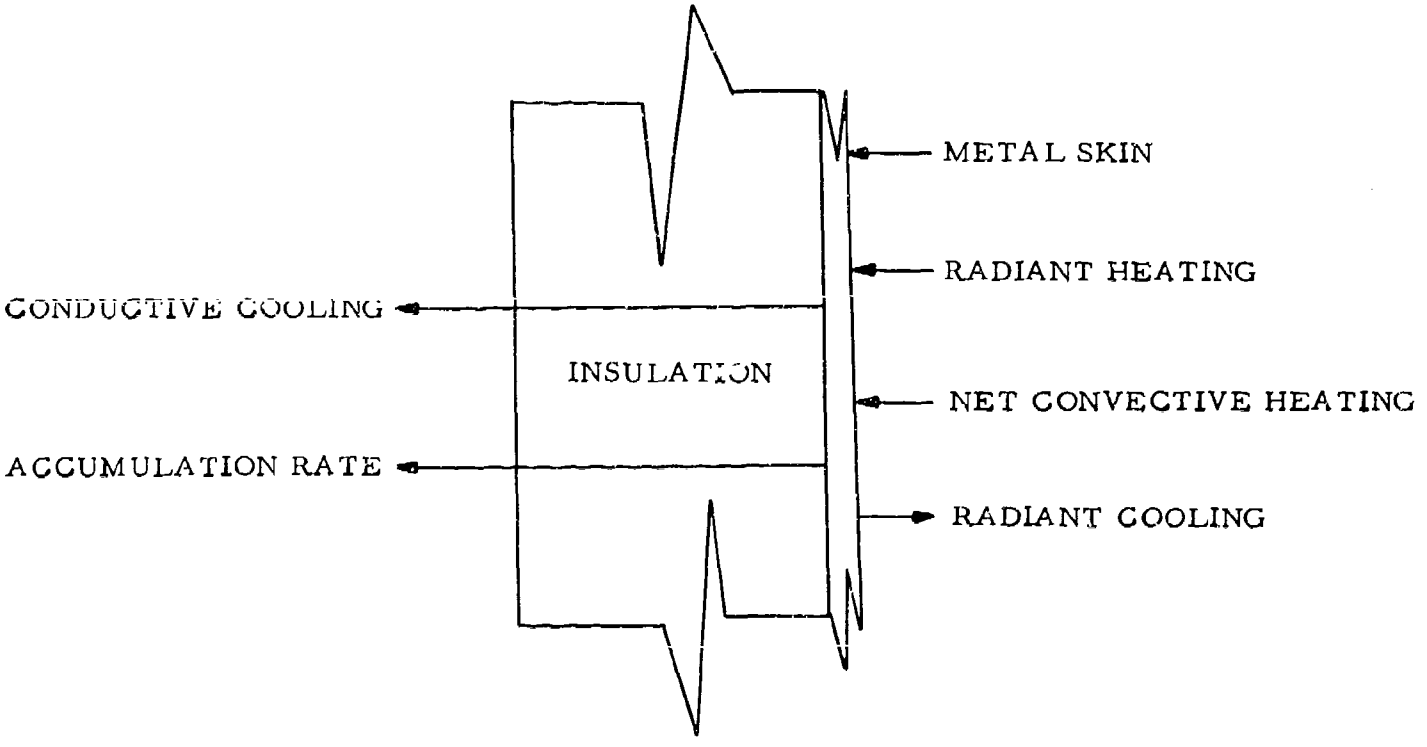

FIG. 16 SIMPLIFIED MODEL OF AIRCRAFT SKIN HEATING (NOT TO SCALE)

Verification of the Mathematical Model

Stainless Steel Tests - The results of calculations made employing the mathematical model based on the 0.031-inch-thick stainless steel skin are presented in Figure 17. The solid curve is the result of calculations made at specific time intervals until the skin temperature reached approximately 1500°F. The parametric data presented in Table 4-I, Appendix IV, were used to obtain the calculated results. For comparison of the calculated results with the experimental data obtained for the 0.031-inch stainless steel tests, the curve has been superimposed on Figure 6.

It is noteworthy that these data were taken from Test No. 2 in which the most rapid temperature rise was recorded. The slower temperature rise during the other tests was due to poor fire coverage of the fuselage which was caused by adverse wind conditions during these tests.

Figure 18 shows the calculated fire damage time for aluminum aircraft skins as a function of the temperature rise for stainless steel. Curves are shown for skin temperatures of 900°F and 1200°F. The two data points shown are adjusted values taken from Figure 17. It will be noted that they are in good agreement with the data predicted by the mathematical model.

Aluminum Panel Tests - The results of the calculations made employing the mathematical model for aluminum aircraft skins are shown by the curve in Figure 19 for a thickness of 0.020 inch and by the curve in Figure 20 for a thickness of 0.090 inch. The experimental data from the fire tests are shown on each of the figures as points. The open points are the actual temperature measurements, and the solid points were adjusted as described for the stainless steel tests.

In Figure 21, the aluminum panel thickness is plotted as a function of time to reach the two temperature levels which constitute the boundaries of the melting range. For the aluminum alloys employed in these tests (2024-T3 and 7075-T6), the beginning temperature was approximately 900°F and the ending temperature approximately 1200°F. The calculated curves and experimental points show reasonable agreement although there are some deviations representative of the 0.090-inch-thick aluminum. The 0.090-inch-thick aluminum panel shows the widest deviation from the calculated curve as the temperature approaches the upper limit for the melting range.

The results of comparisons of stainless steel and aluminum calculations and experimental test results indicate that the calculations are adequate for use as a method of estimating the time required for damage to occur to an aircraft fuselage in an accident involving instant

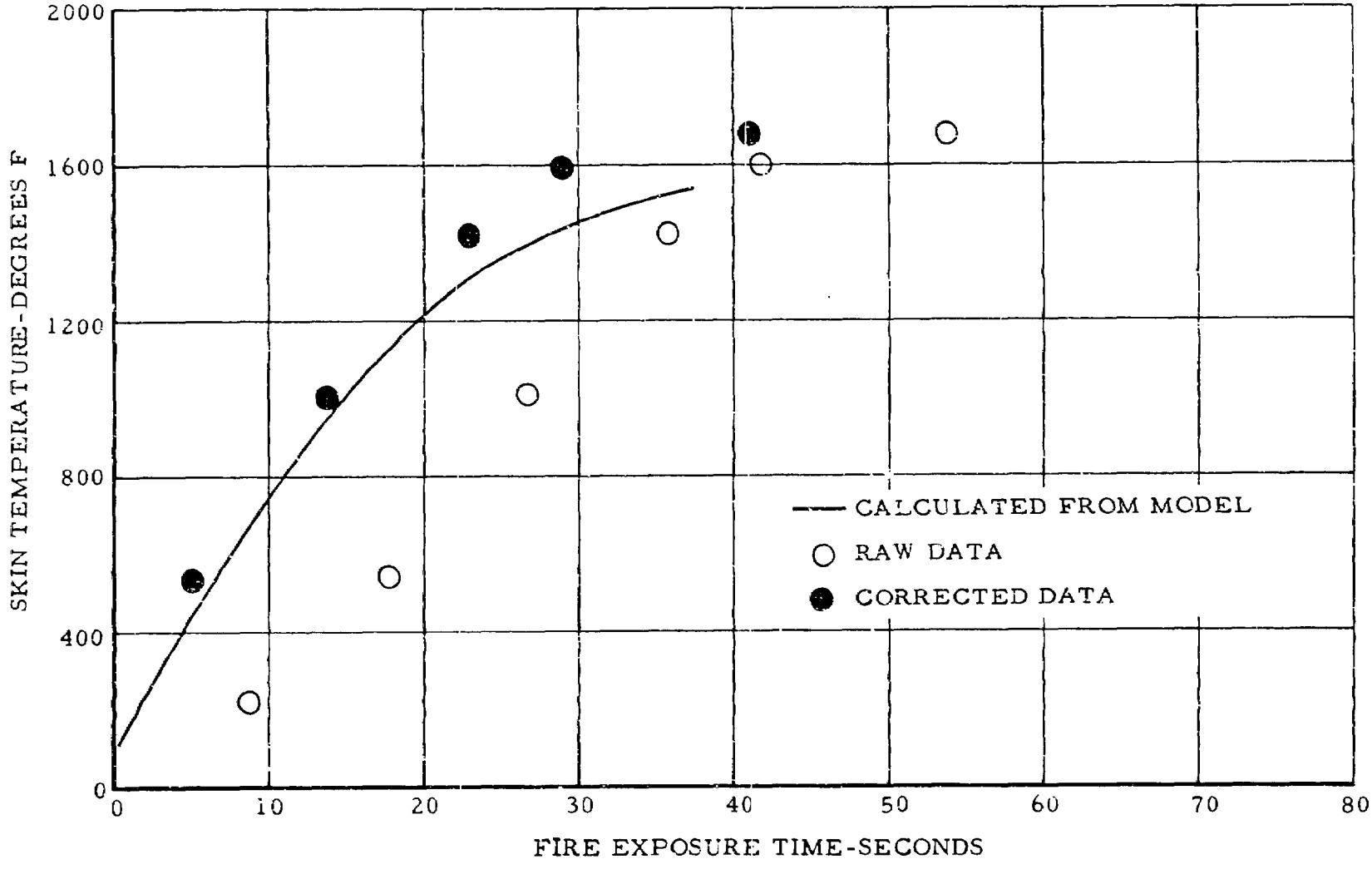

FIG. 17 SKIN TEMPERATURE FOR 0.031-INCH STAINLESS STEEL AS A FUNCTION OF FIRE EXPOSURE TIME AS CALCULATED FROM THE MODEL

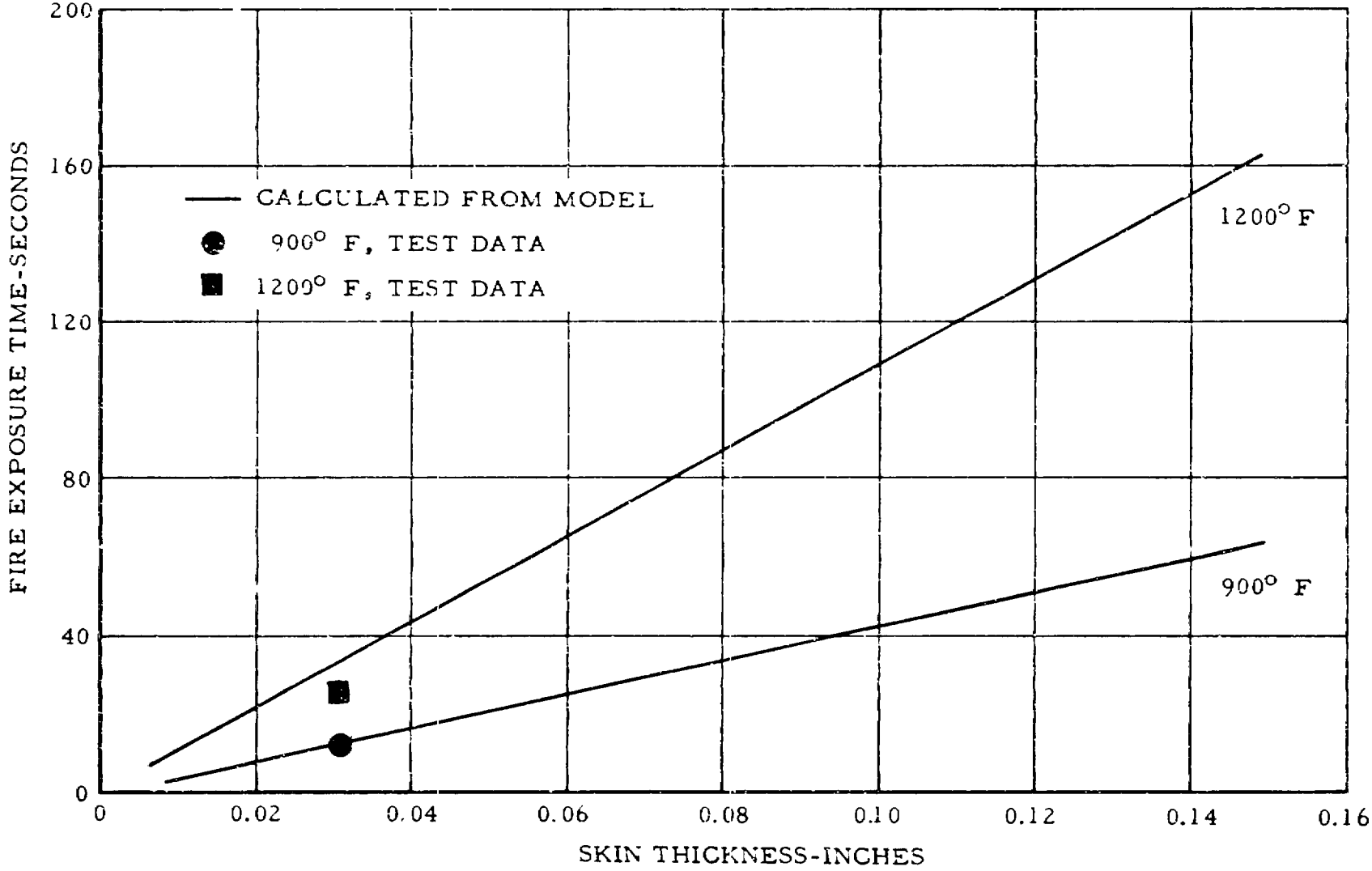

FIG. 18 CALCULATED MELTING TIME FOR ALUMINUM AIRCRAFT SKINS AS A FUNCTION OF THE TEMPERATURE RISE FOR STAINLESS STEEL

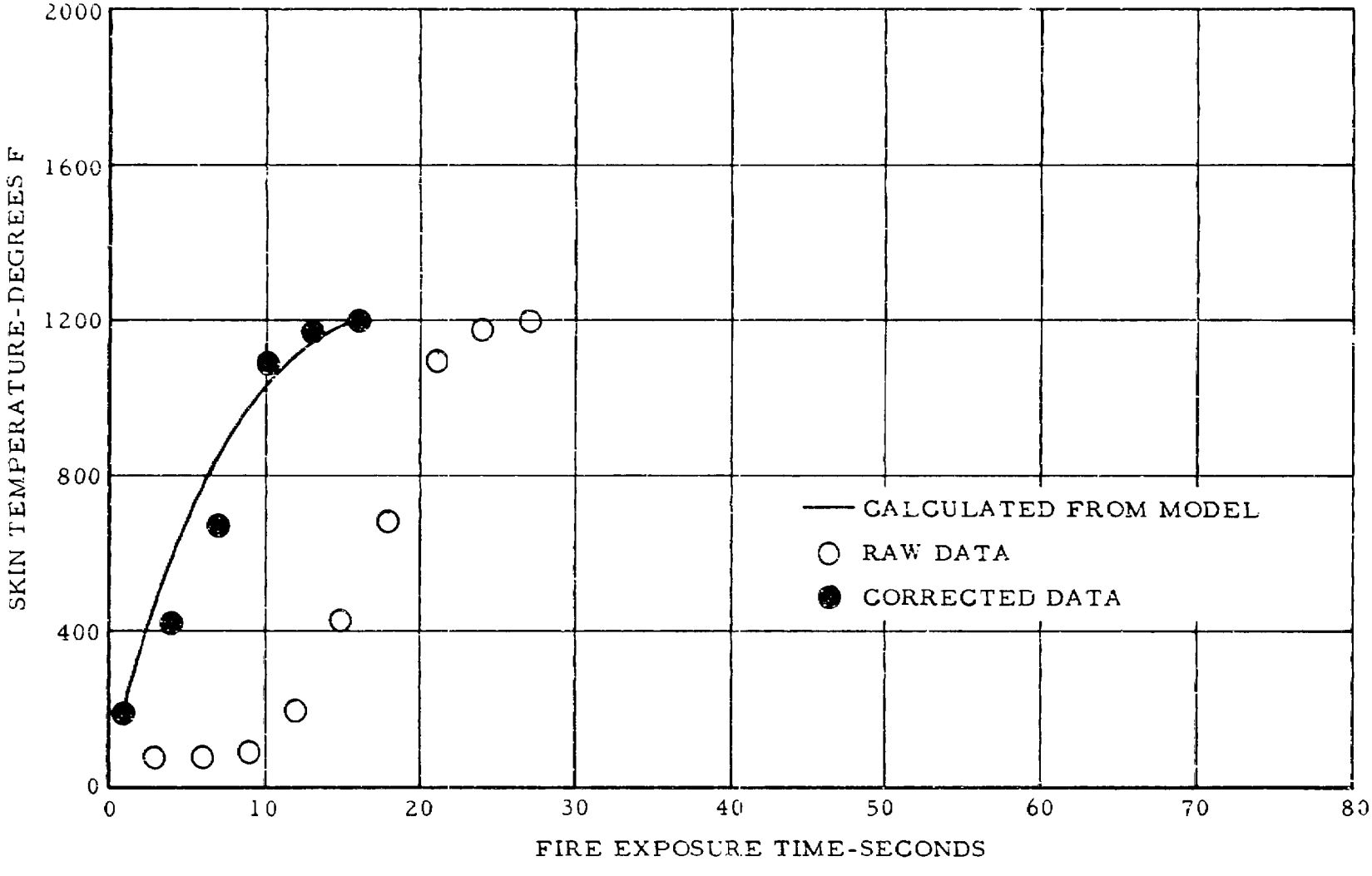

FIG. 19 SKIN TEMPERATURES FOR 0.020-INCH ALUMINUM AS A FUNCTION OF FIRE EXPOSURE TIME

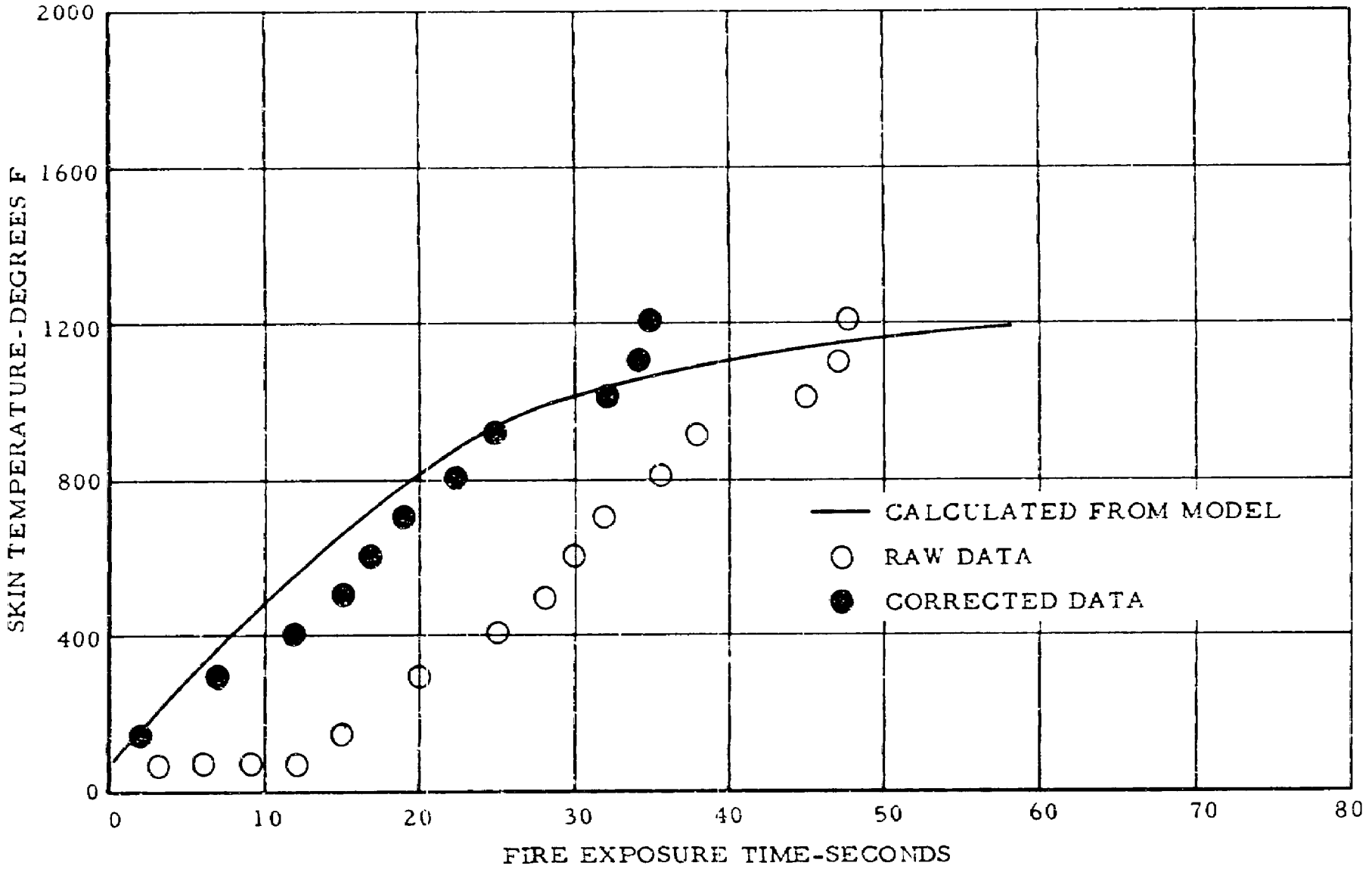

FIG. 20 SKIN TEMPERATURE FOR 0.090-INCH ALUMINUM AS A FUNCTION OF FIRE EXPOSURE TIME

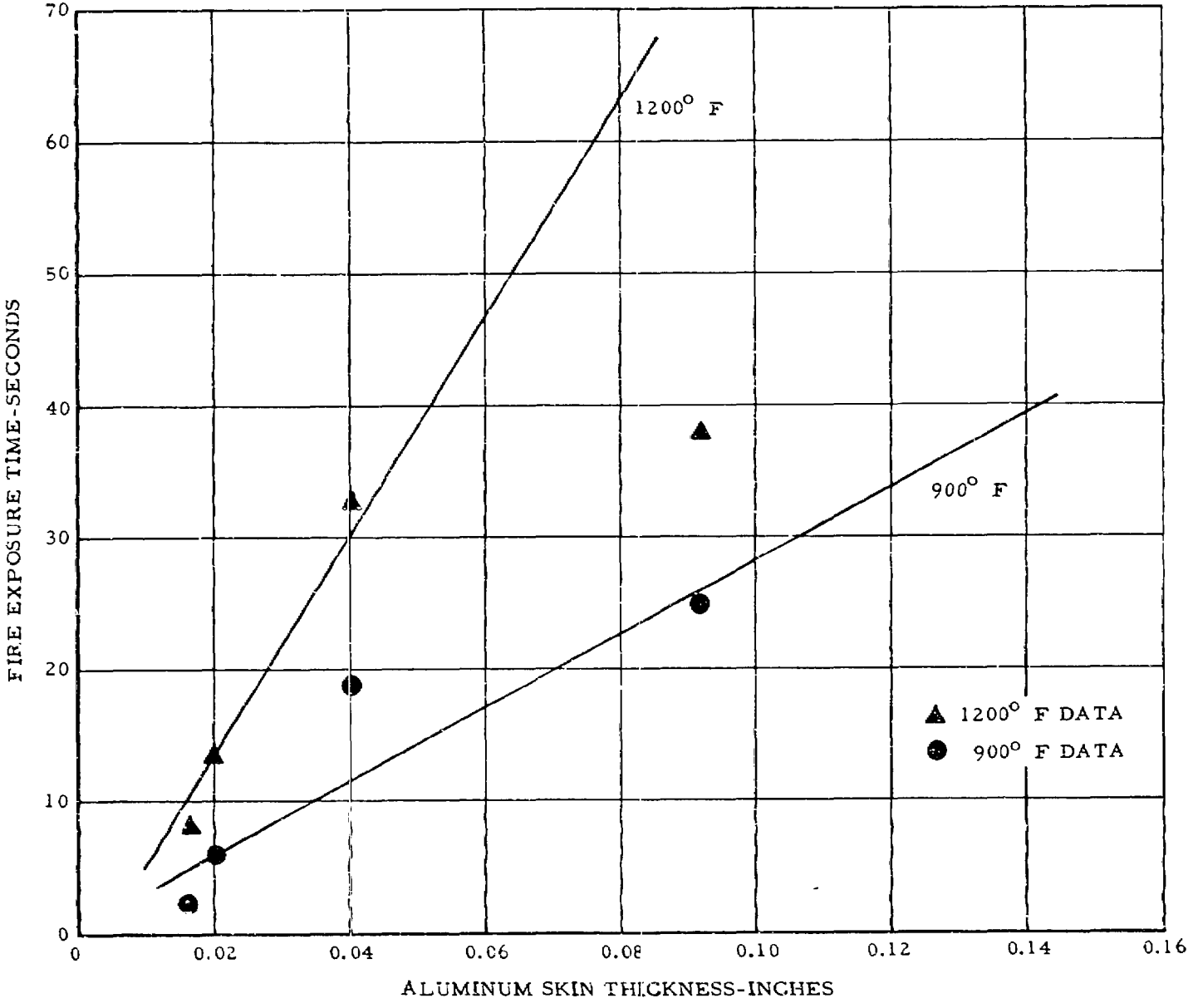

FIG. 21 MELTING TIME FOR DIFFERENT THICKNESSES OF AIRCRAFT ALUMINUM AS A FUNCTION OF FIRE EXPOSURE TIME

extreme fire conditions. The total elapsed time necessary for an aircraft skin to melt can be calculated if the skin thickness is known. However, for most aircraft, the skin thickness varies along the fuselage with the structural requirements.

Figure 22 shows the minimum aircraft skin thickness as a function of the gross weight of the aircraft. The curve shows approximate values for aircraft of several manufacturers which range from small single-engine aircraft to intercontinental jet aircraft. It should be emphasized that Figure 22 gives the minimum skin thickness for a given aircraft gross weight and the maximum skin thickness on the same aircraft may be several times the minimum.

The curve in Figure 23 was developed from data taken from Figures 21 and 22 and shows the time required for an aircraft skin to melt as a function of the aircraft gross weight. The procedure was to plot the minimum skin thickness of the aircraft taken from Figure 22 and the fire damage time as the time required to reach 1200^{0}F from Figure 21. The curve in Figure 23 shows that the aircraft skin melting time varies from about 10 seconds for small aircraft to nearly 40 seconds for the larger aircraft. These melting times are based on immediate fire involvement and a large fire so they represent the minimum time available for fire suppression before the fire penetrates the cabin. Should ignition not occur immediately or if an appreciable time is required for the fire to build up, this additional time would be available for fire suppression. However, neither of these conditions can be relied upon in an aircraft incident. Therefore, fire suppression techniques and equipment should be designed for effective operation within the minimum time available or modifications in aircraft construction should be considered to extend the minimum fire damage time if protection to passengers and crew is to be obtained.

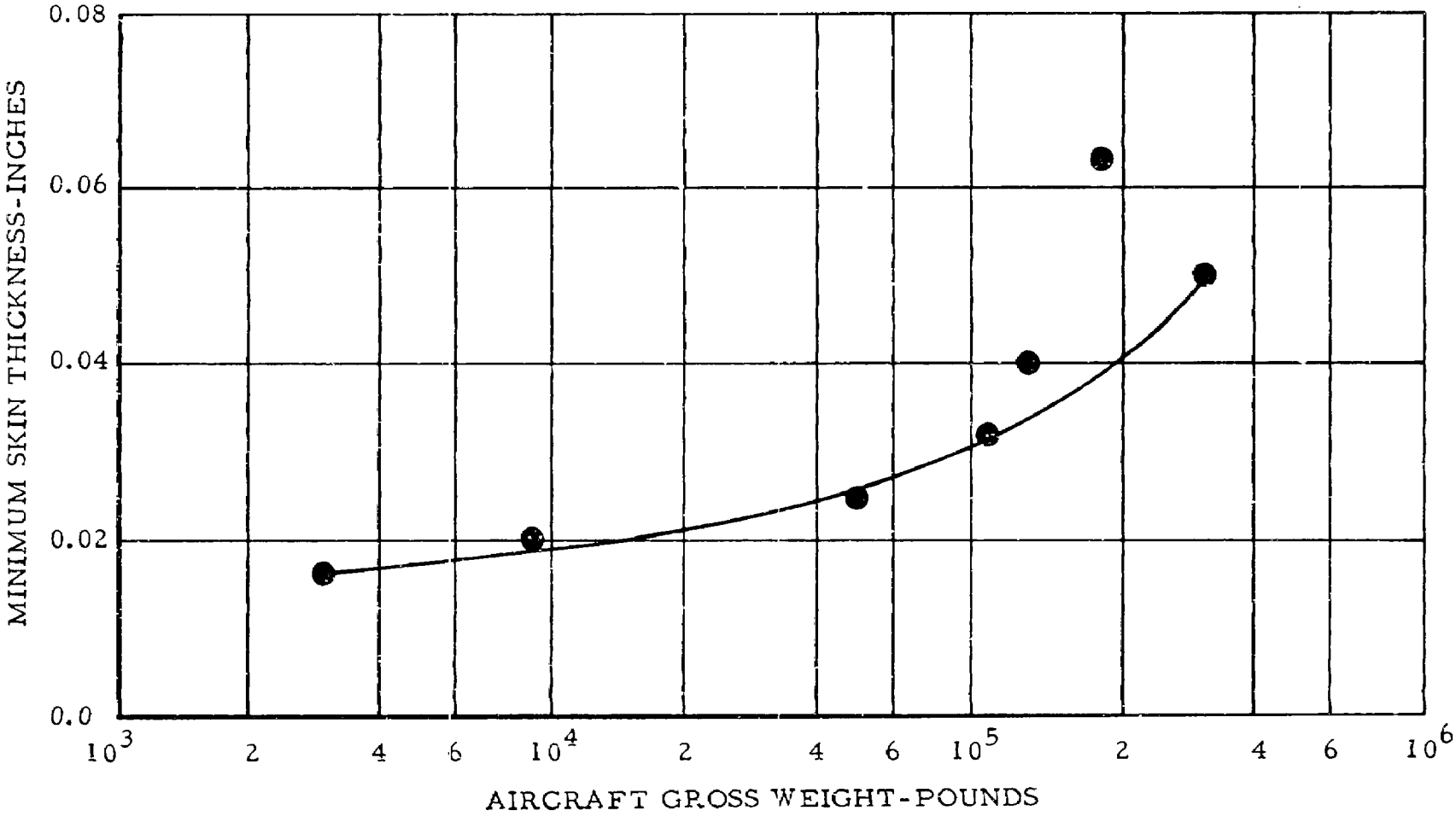

FIG. 22 MINIMUM SKIN THICKNESS OF SOME CURRENT COMMERCIAL AIRCRAFT

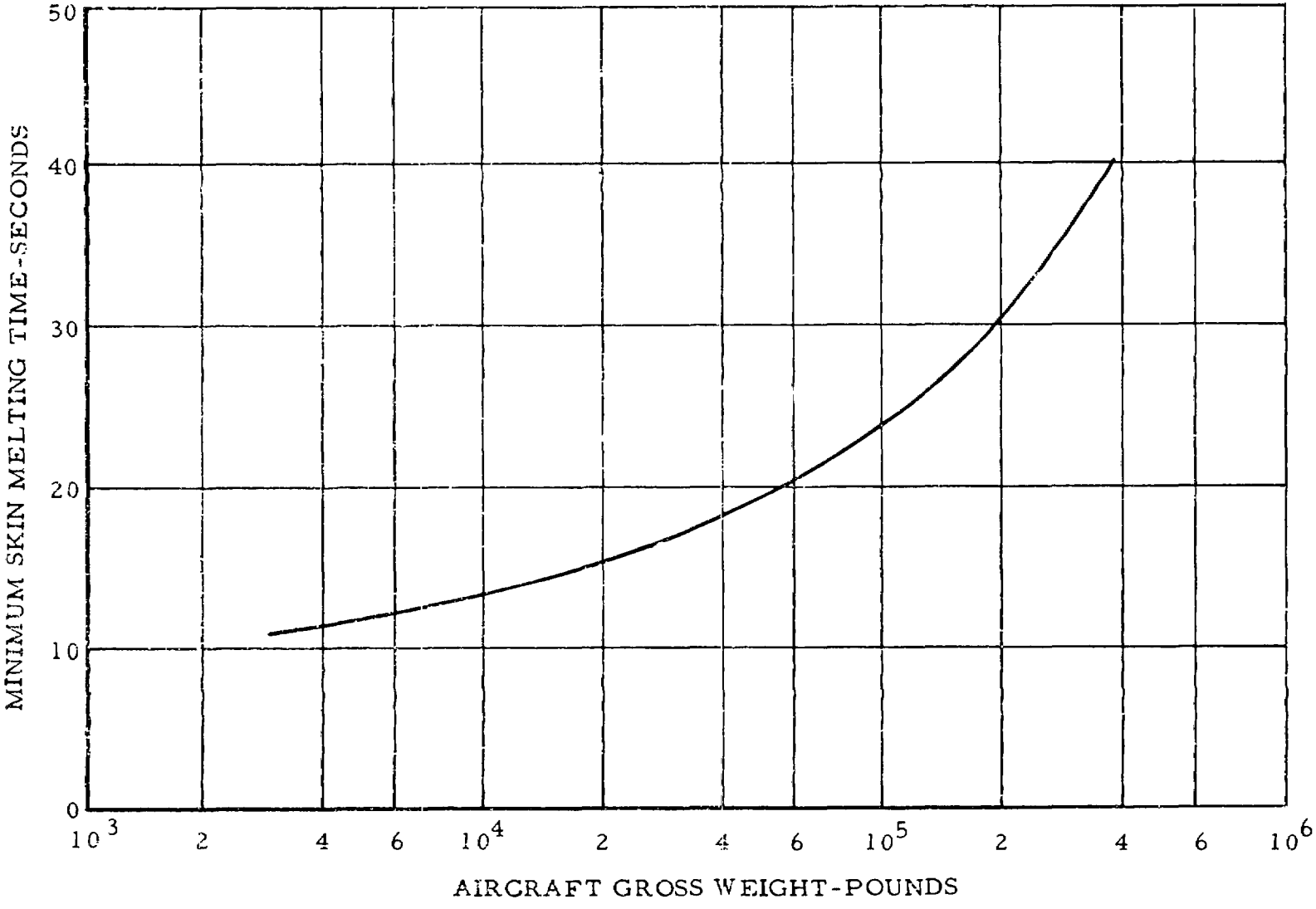

FIG. 23 MINIMUM SKIN MELTING TIME AS A FUNCTION OF THE GROSS WEIGHT OF THE AIRCRAFT

SUMMARY OF RESULTS

The results obtained from theoretical considerations of heat transfer and large-scale fire tests are:

1. The calculated melting times obtained using the mathematical model for four different thicknesses of aircraft aluminum show acceptable agreement with the experimental results obtained from the large-scale fire tests.

2. The melting time of four aluminum panels exposed to severe fire conditions varied from approximately 8 seconds for the 0.016-inch-thick aluminum to 38 seconds for the 0.090-inch-thick aluminum.

3. A simulated spill fire 10 feet wide and 40 feet long located 10 feet from the stainless-steel-covered fuselage on the upwind side indicated that 0.031-inch-thick aircraft aluminum would melt in approximately 25 seconds.

4. The effect of wind on pool fires significantly increased the destructive range of the fire plume downwind from the actual spill boundary as a result of flame trailing.

CONCLUSIONS

Based on the results of thermal calculations and experiments, it is concluded that:

1. The mathematical model developed in this report is adequate to predict the melting time of aircraft aluminum paneling under severe fire conditions.

2. The insulated aluminum fuselage skin of current aircraft provides low resistance to external fuel fire. The melting time of fuselage panels and subsequent fire entry into the cabin interior from fires of maximum severity is on the order of 10 to 40 seconds depending on skin thickness.

3. A fuel spill fire remote and on the upwind side of an aircraft fuselage may inflict severe fire damage as a result of the flame-trailing phenomenon.

RECOMMENDATIONS

Based upon full-scale fire tests and mathematical methods, it is recommended that:

1. The mathematical model and the curves developed in this report be employed to estimate the approximate melting time for aircraft aluminum of different thicknesses when exposed to aircraft fuel fires of maximum severity.

2. The data and information contained in this report for the time required for the melting of fuselage skin, under severe fire conditions, be used as the primary criteria for estimating airport firefighting equipment requirements.

3. Consideration be given to the possibility of extensive flame spread around an aircraft fuselage as a result of flame trailing under variable wind conditions.

4. Studies be conducted on means of extending occupant survival time by encapsulating the aircraft cabin interior in a flame resistant barrier.

REFERENCES

1. Welker, J. R. and Sliepcevich, C. M., The Effect of Wind on Flames, Technical Report No. 2, NBS Contract No. CST-1142, University of Oklahoma Research Institute, Norman, Oklahoma (November 1965).

2. Mickley, H. S., Sherwood, T. K., and Reed, C. E., Applied Mathematics in Chemical Engineering, Second Edition, McGraw-Hill (1957).

3. Copley, J. A., An Analytical Method for Predicting the Temperature-Time History of a Hollow Cylinder Enveloped in Flames, Technical Report No. 2073, U.S. Naval Weapons Laboratory, Dahlgren, Virginia (December 1966). AD804084.

4. Neill, D. T., Heat Transfer from Uncontrolled Buoyant Diffusion Flames, Ph. D. Thesis, University of Oklahoma, Norman, Oklahoma (1968).

5. Perry, R. H., Chilton, C. H., and Kirkpatrick, S. D., Editions, Chemical Engineers Handbook, Fourth Edition, McGraw-Hill, New York (1963).

6. Stull, D. C., Edition, JANAF Thermocouple Tables, AF Contract No. AF04(611)-7554.

ACKNOWLEDGMENT

Appreciation is expressed to Dr. J. Reed Welker of University Engineers, Inc., Norman, Oklahoma, for the mathematical interpretation of the fuselage fire damage time.

APPENDIX I

STAINLESS-STEEL-COVERED FUSELAGE TESTS, THERMOCOUPLE AND RADIOMETER DATA

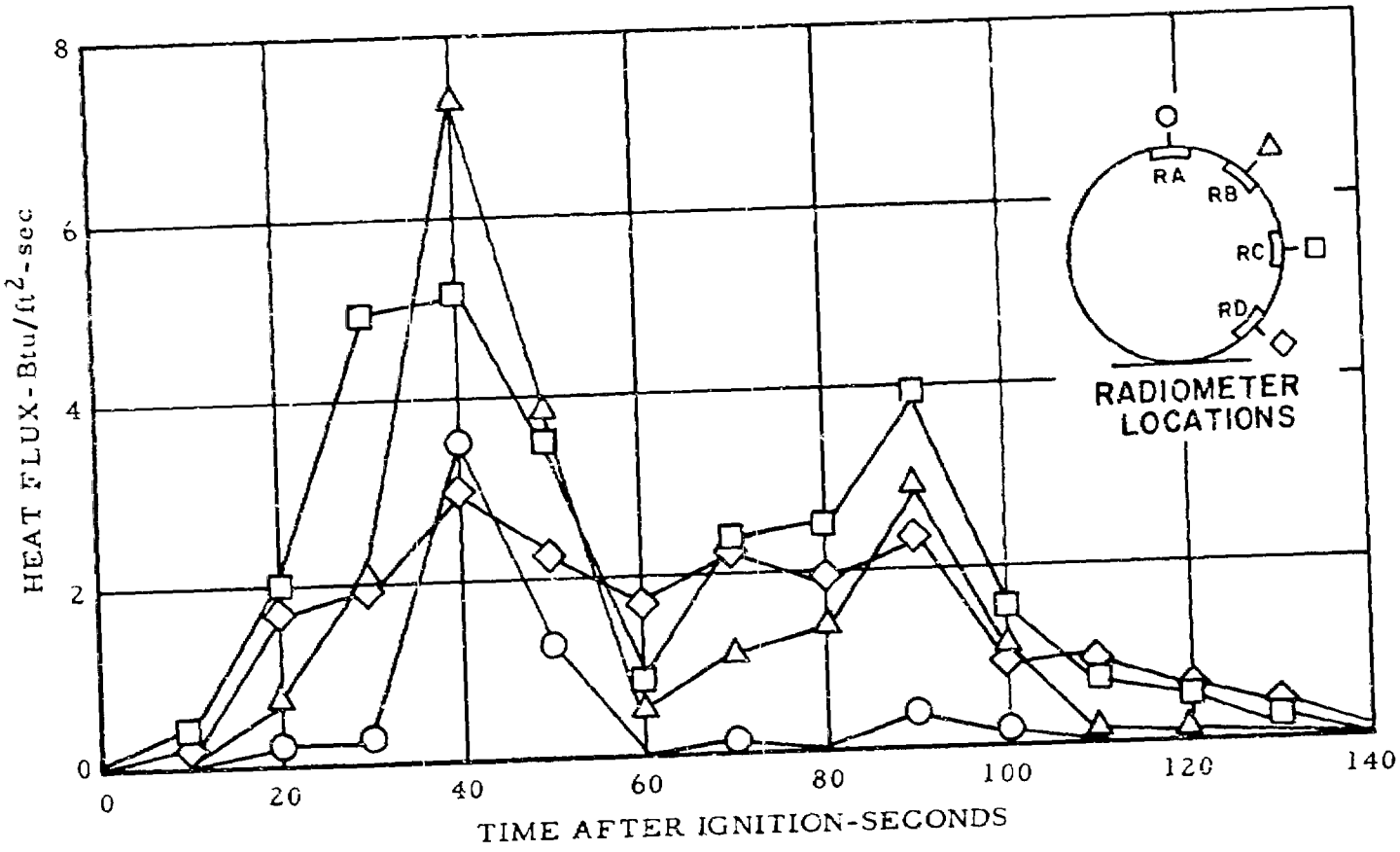

FIG. 1.1 TEST NO. 1 - RADIOMETER DATA FOR STAINLESS-STEEL-COVERED FUSELAGE

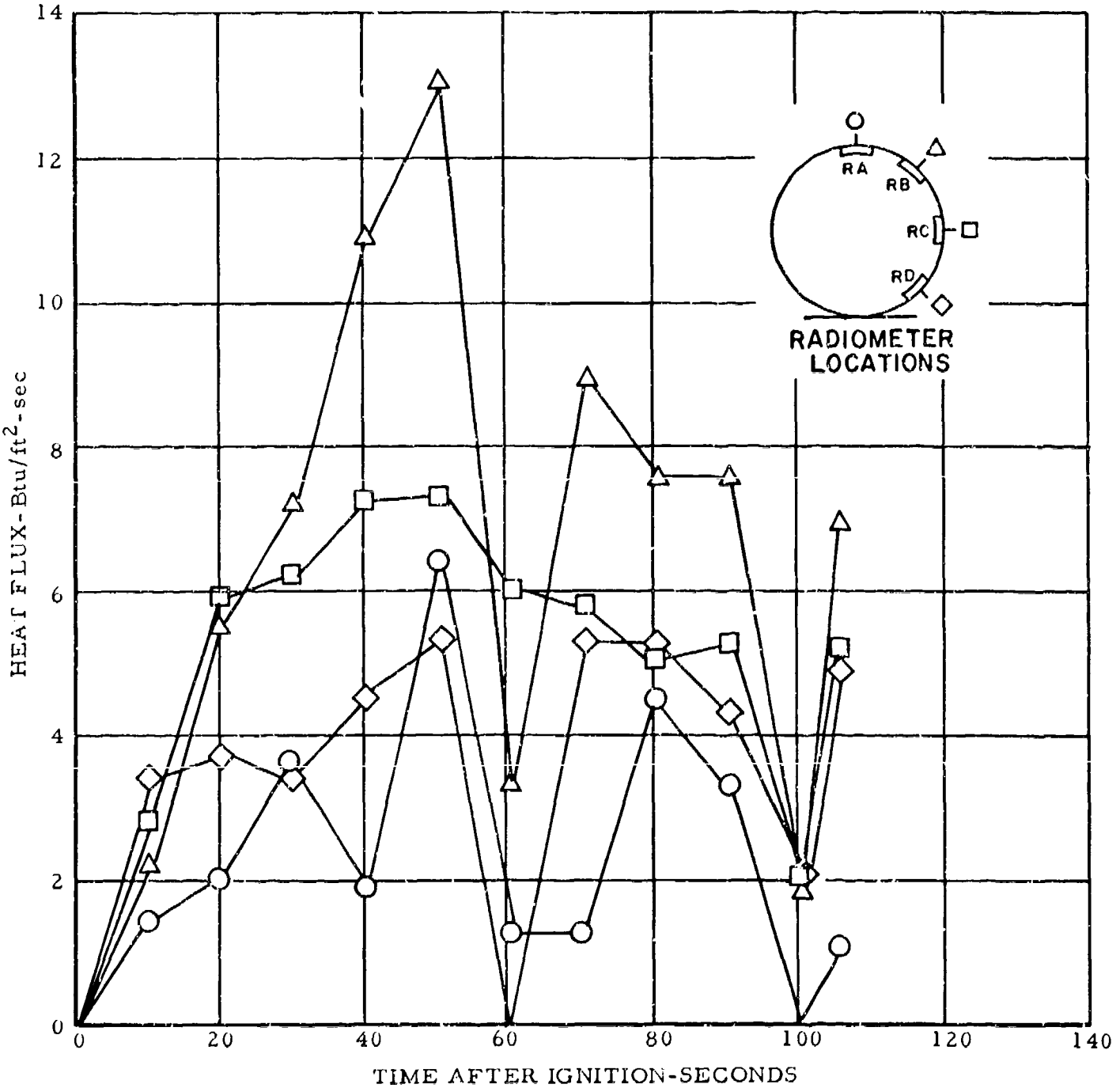

FIG. 1.2 TEST NO. 2 - RADIOMETER DATA FOR STAINLESS-STEEL-COVERED FUSELAGE

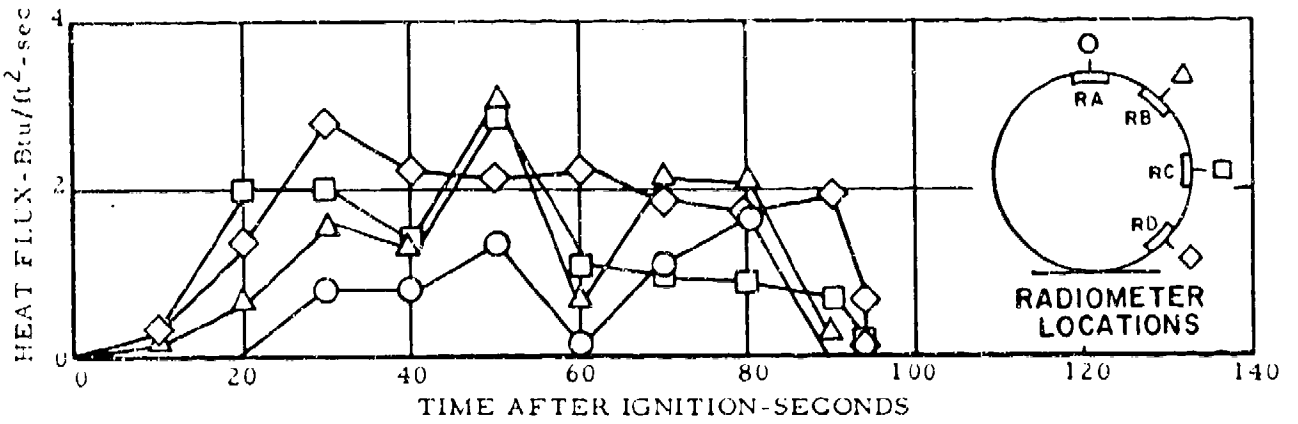

FIG. 1.3 TEST NO. 3 - RADIOMETER DATA FOR STAINLESS-STEEL-COVERED FUSELAGE

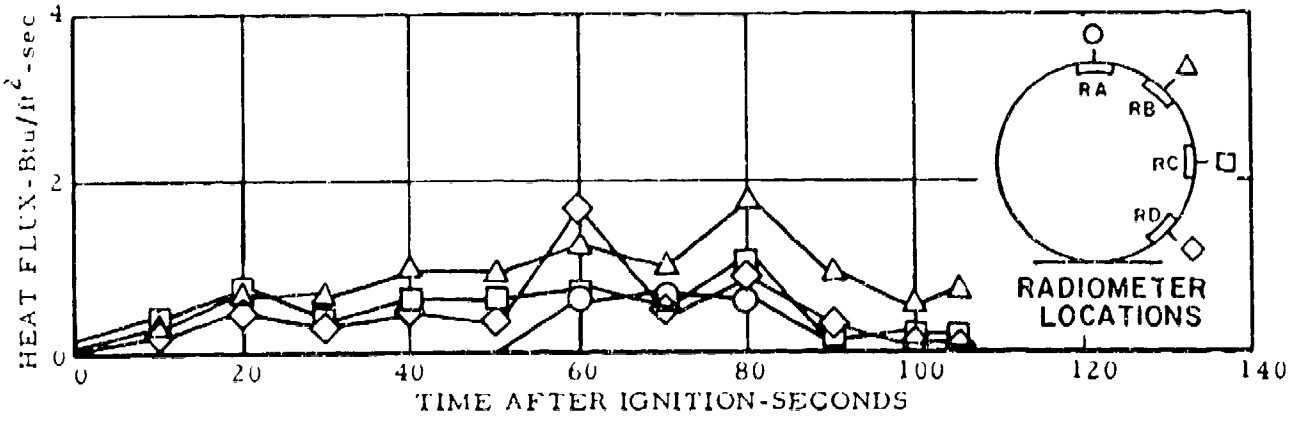

FIG. 1.4 TEST NO. 4 - RADIOMETER DATA FOR STAINLESS-STEEL-COVERED FUSELAGE

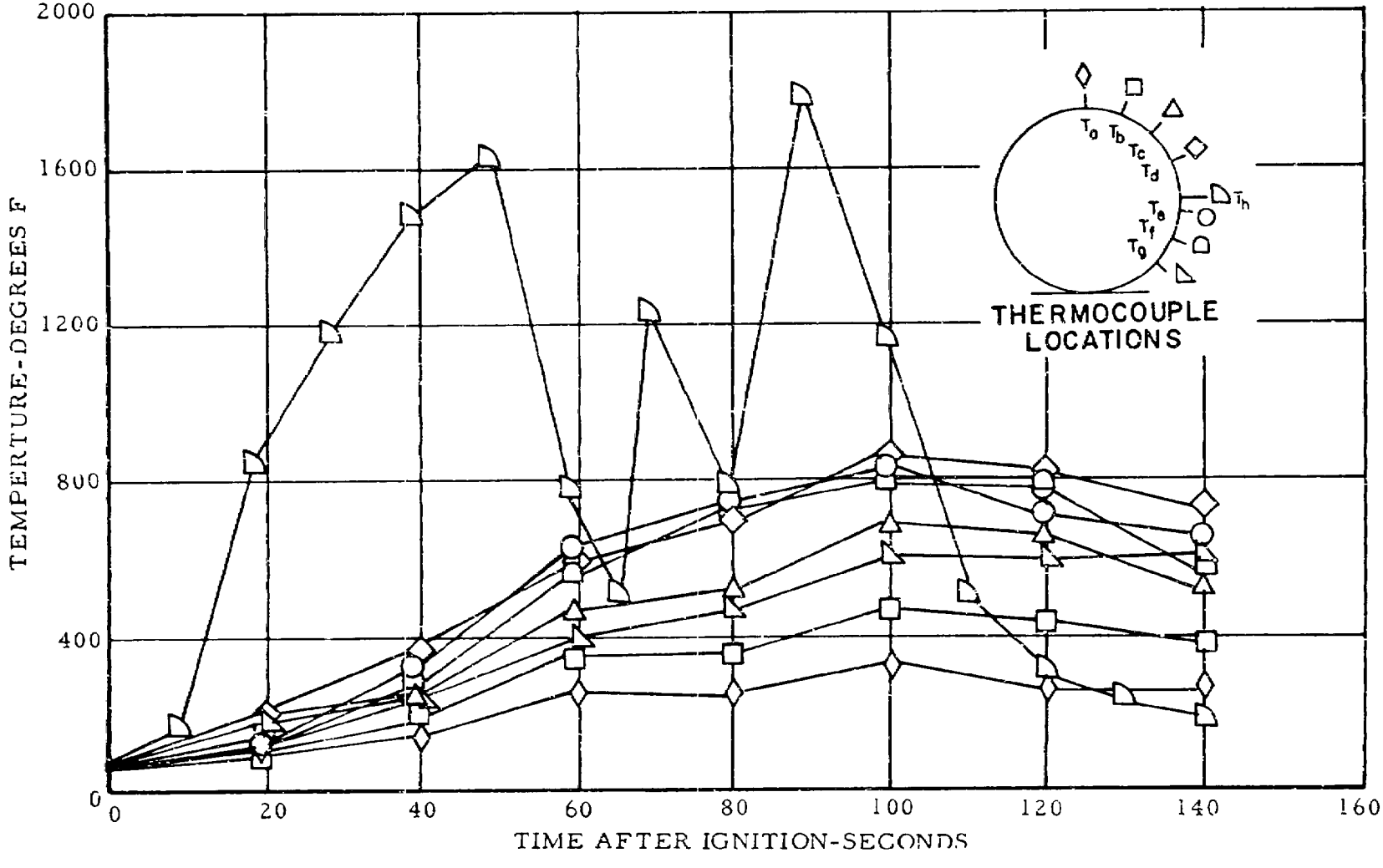

FIG. 1.5 TEST NO. 1 - THERMOCOUPLE DATA FOR STAINLESS-STEEL-COVERED FUSELAGE

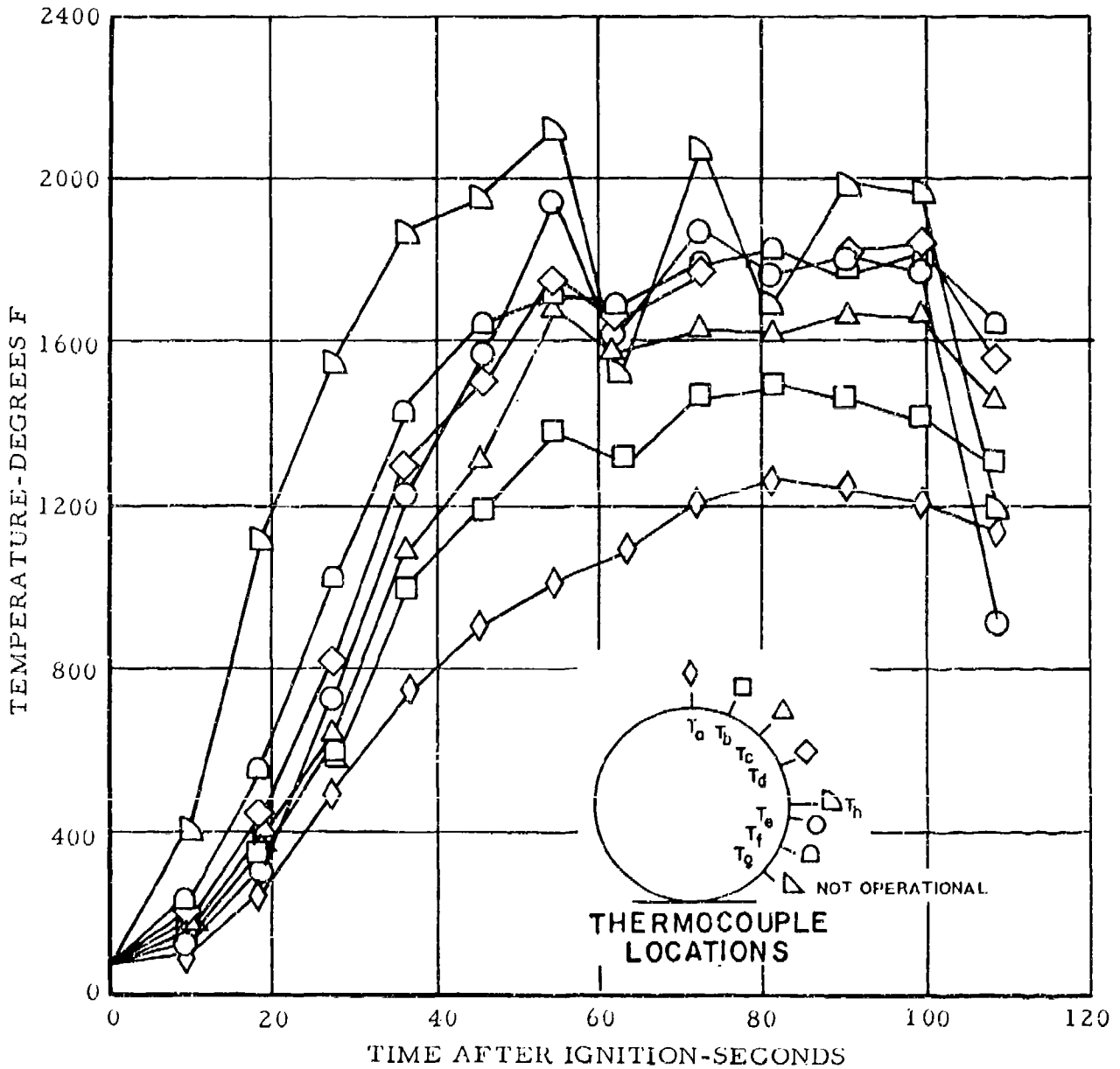

FIG. 1.6 TEST NO. 2 - THERMOCOUPLE DATA FOR STAINLESS-STEEL-COVERED FUSELAGE

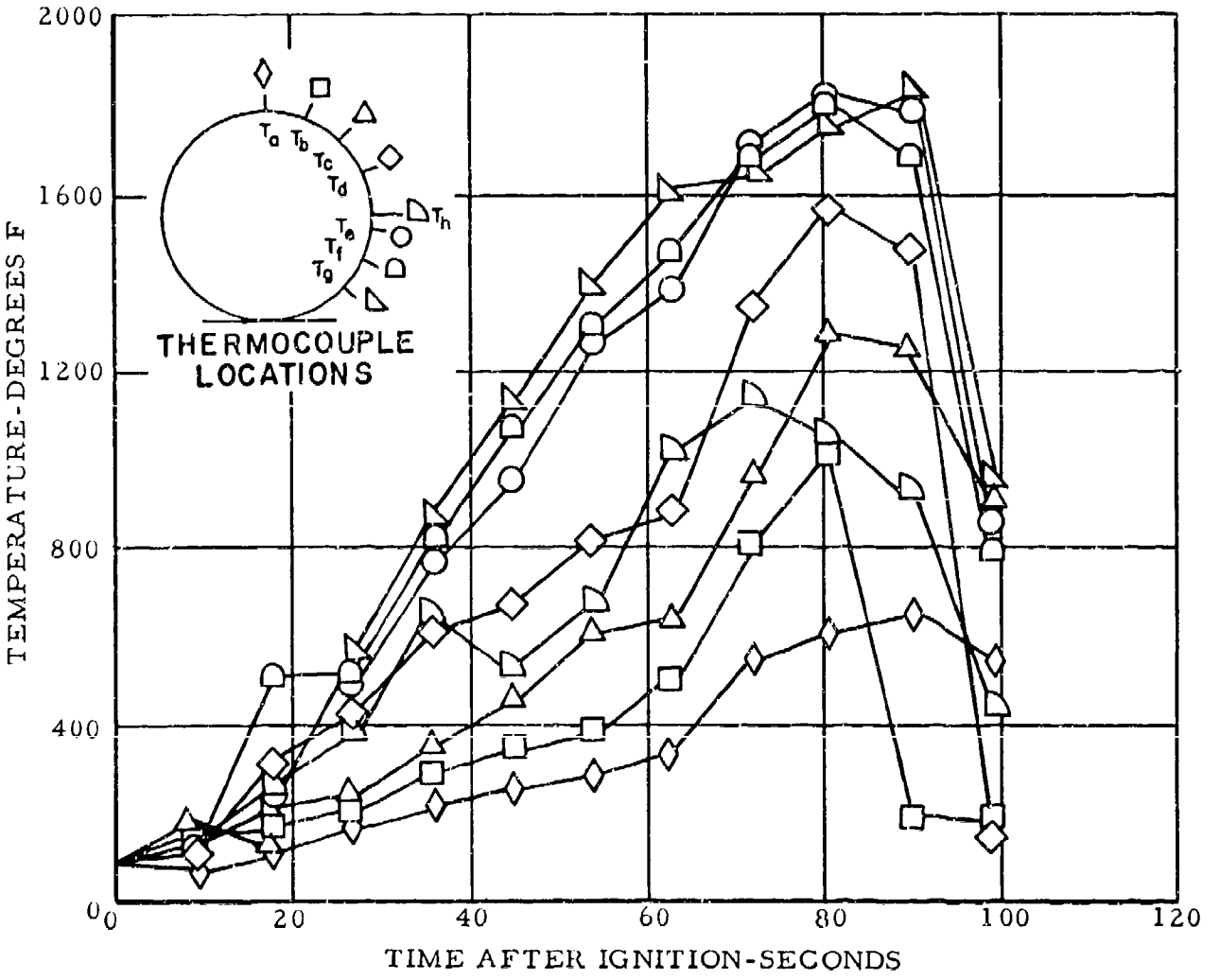

FIG. 1.7 TEST NO. 3 - THERMOCOUPLE DATA FOR STAINLESS-STEEL-COVERED FUSELAGE

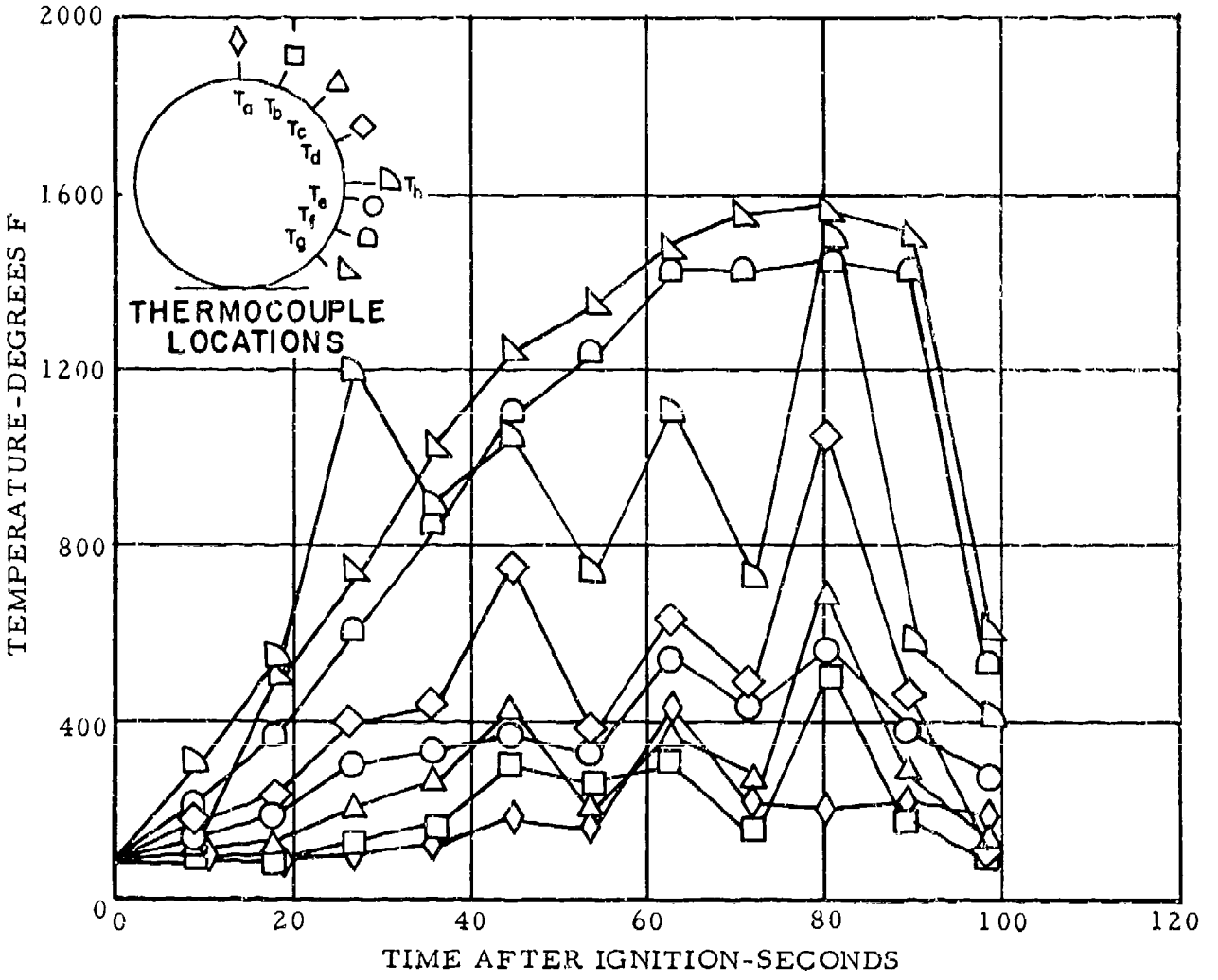

FIG. 1.8 TEST NO. 4 - THERMOCOUPLE DATA FOR STAINLESS-STEEL-COVERED FUSELAGE

APPENDIX II

CRITICAL PHASES OF AN ALUMINUM PANEL TEST

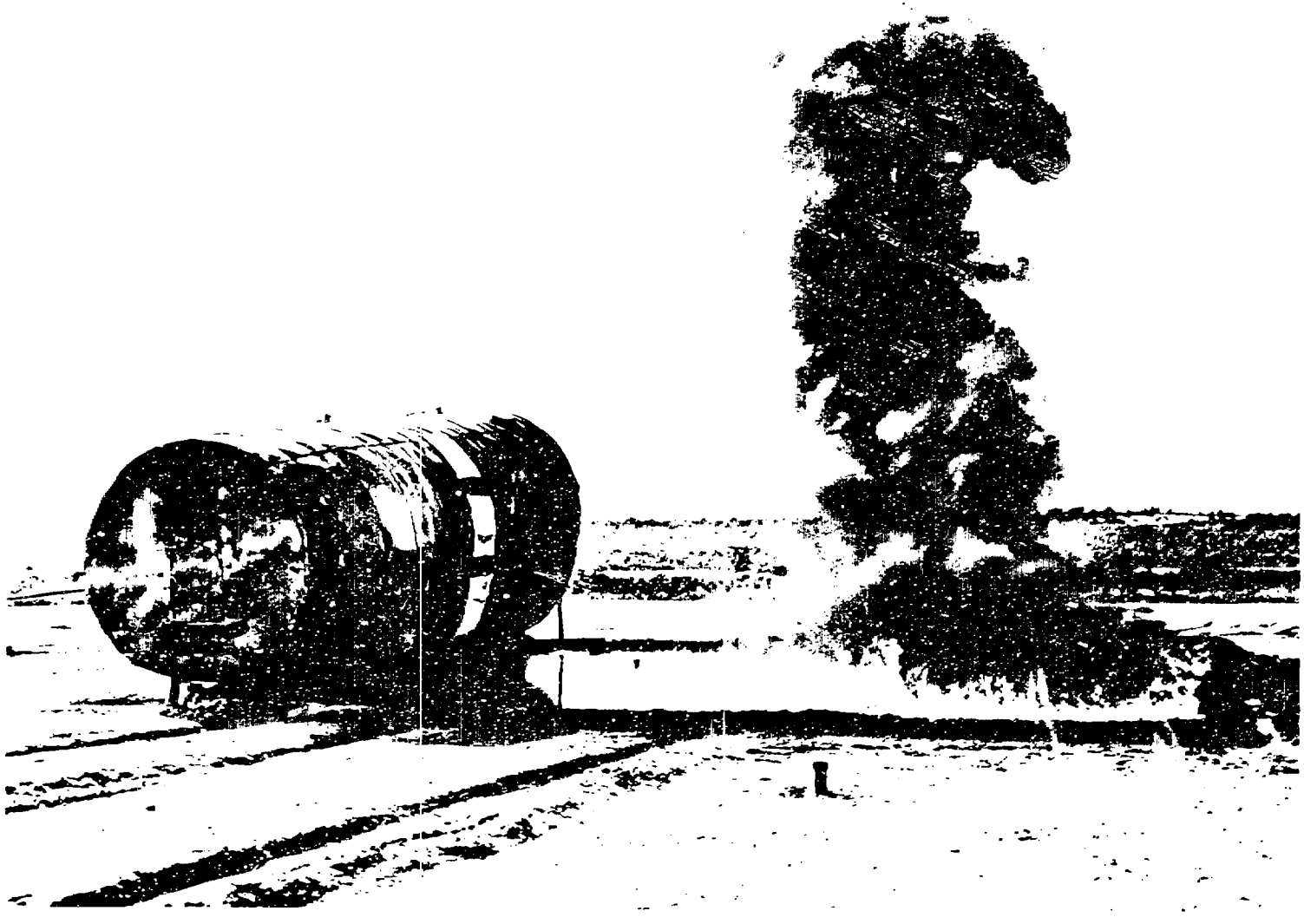

FIG. 2.1 FUEL IGNITION

FIG. 2.2 TIME AFTER IGNITION - 30 SECONDS

FIG. 2.3 FIRE EXTINGUISHMENT OPERATION

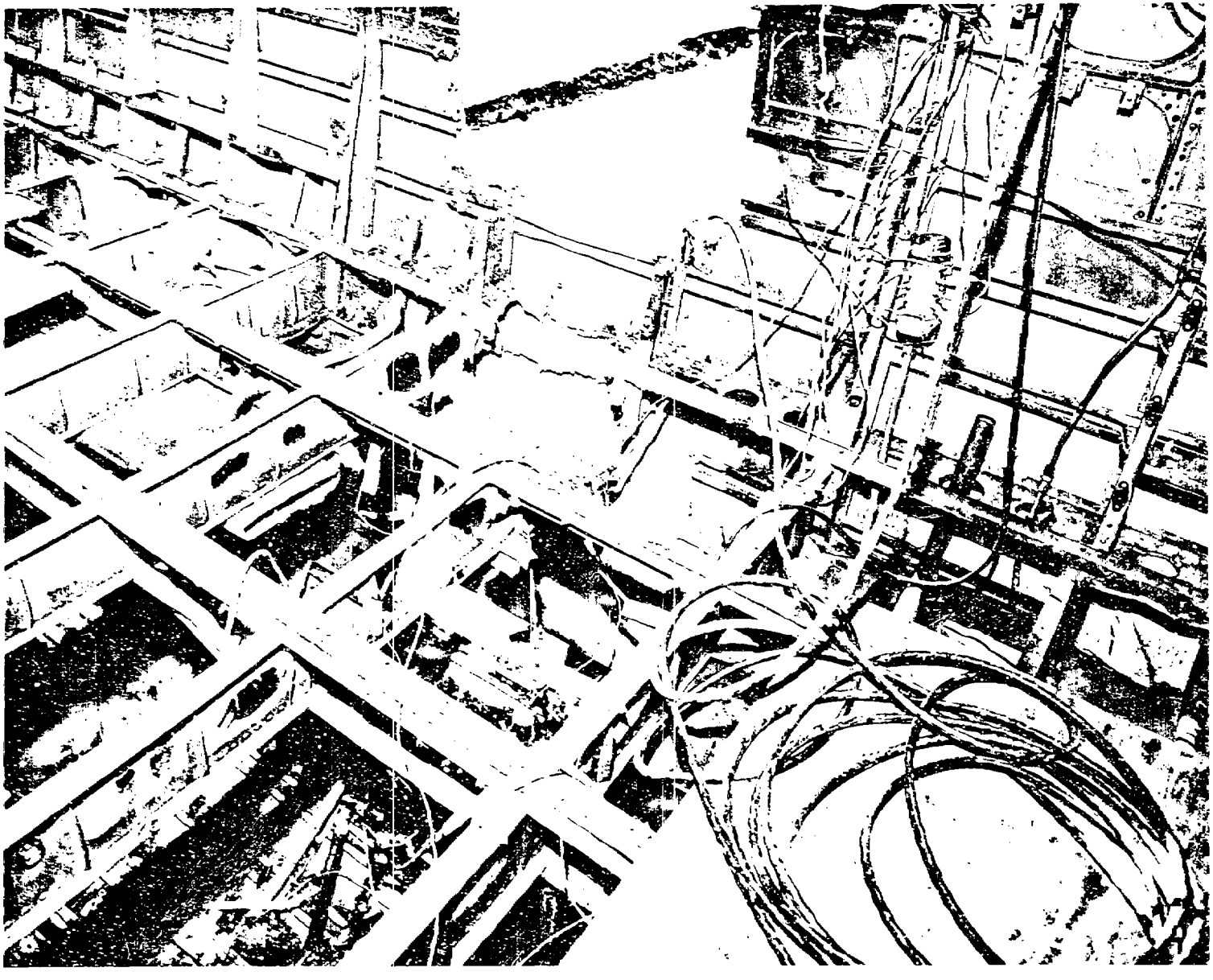

FIG. 2.4 INTERIOR STRUCTURAL DAMAGE AFTER TEST NO. 4

APPENDIX III

ALUMINUM PANEL TESTS, THERMOCOUPLE AND RADIOMETER DATA

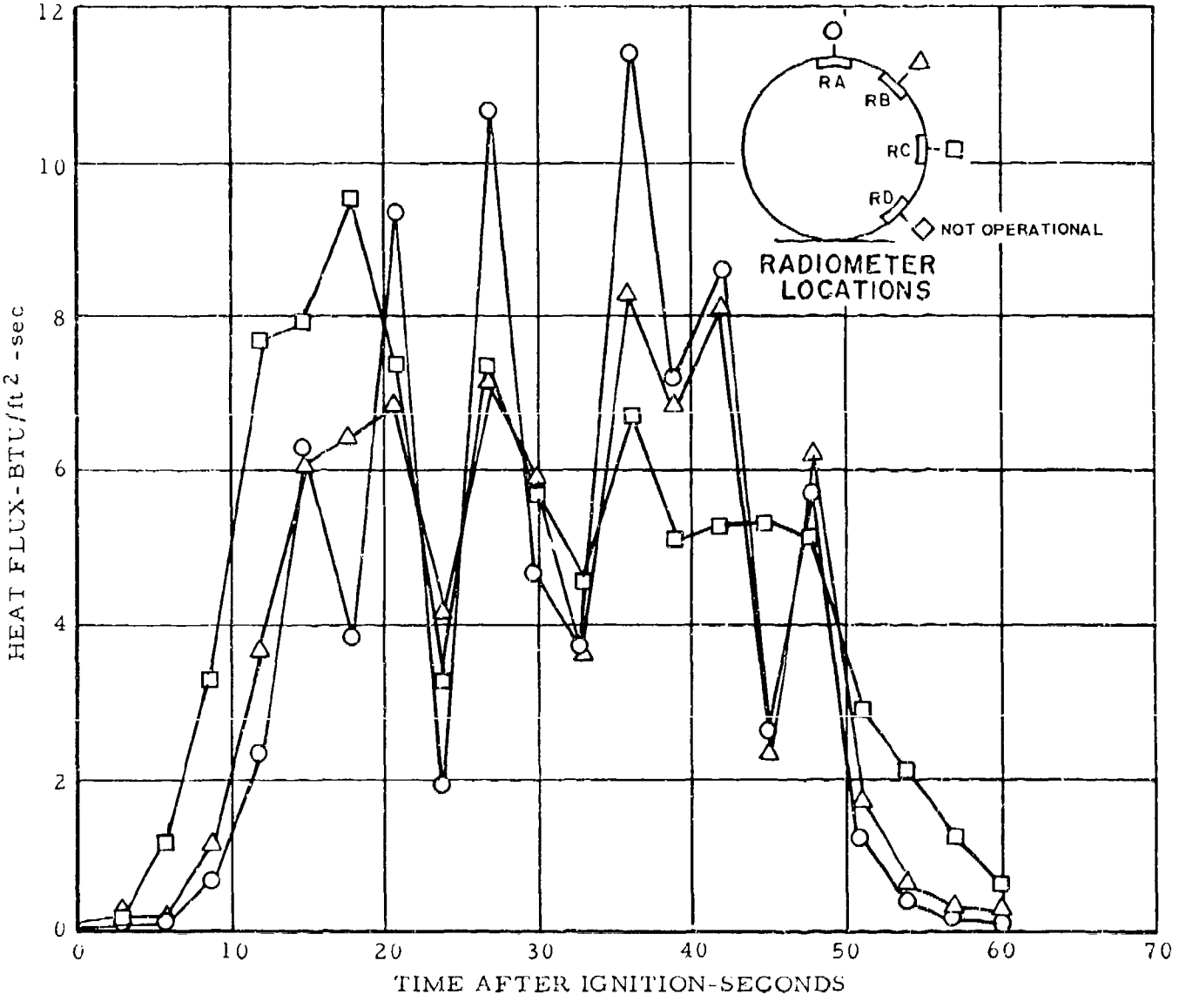

FIG. 3.1 TEST NO. 5 - RADIOMETER DATA FOR ALUMINUM ALLOY 2024-T3 ALCLAD (0.016-INCH THICKNESS)

PRECEDING PAGE BLANK

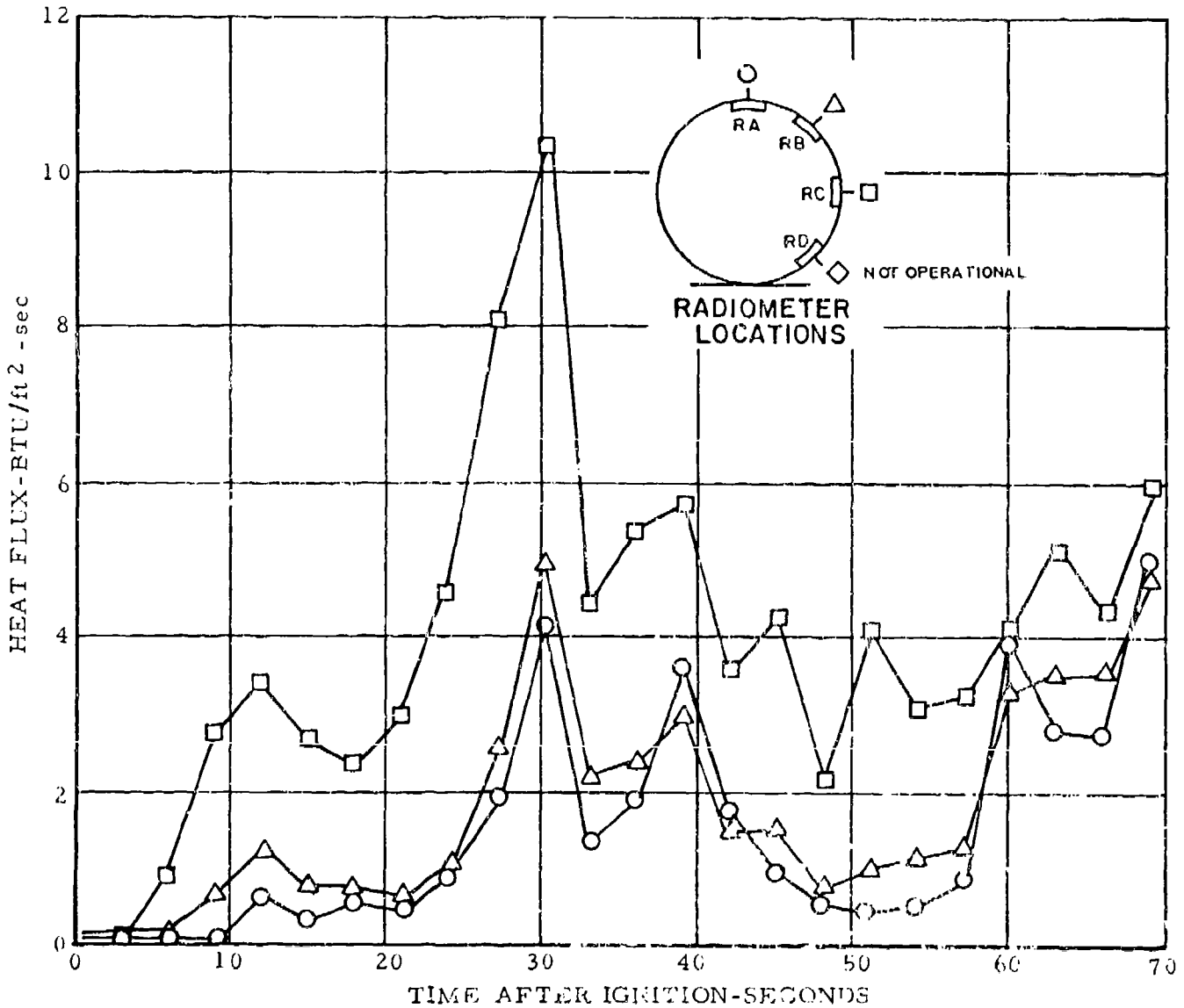

FIG. 3.2 TEST NO. 6 - RADIOMETER DATA FOR ALUMINUM ALLOY 2024-T3 ALCLAD (0.040-INCH THICKNESS)

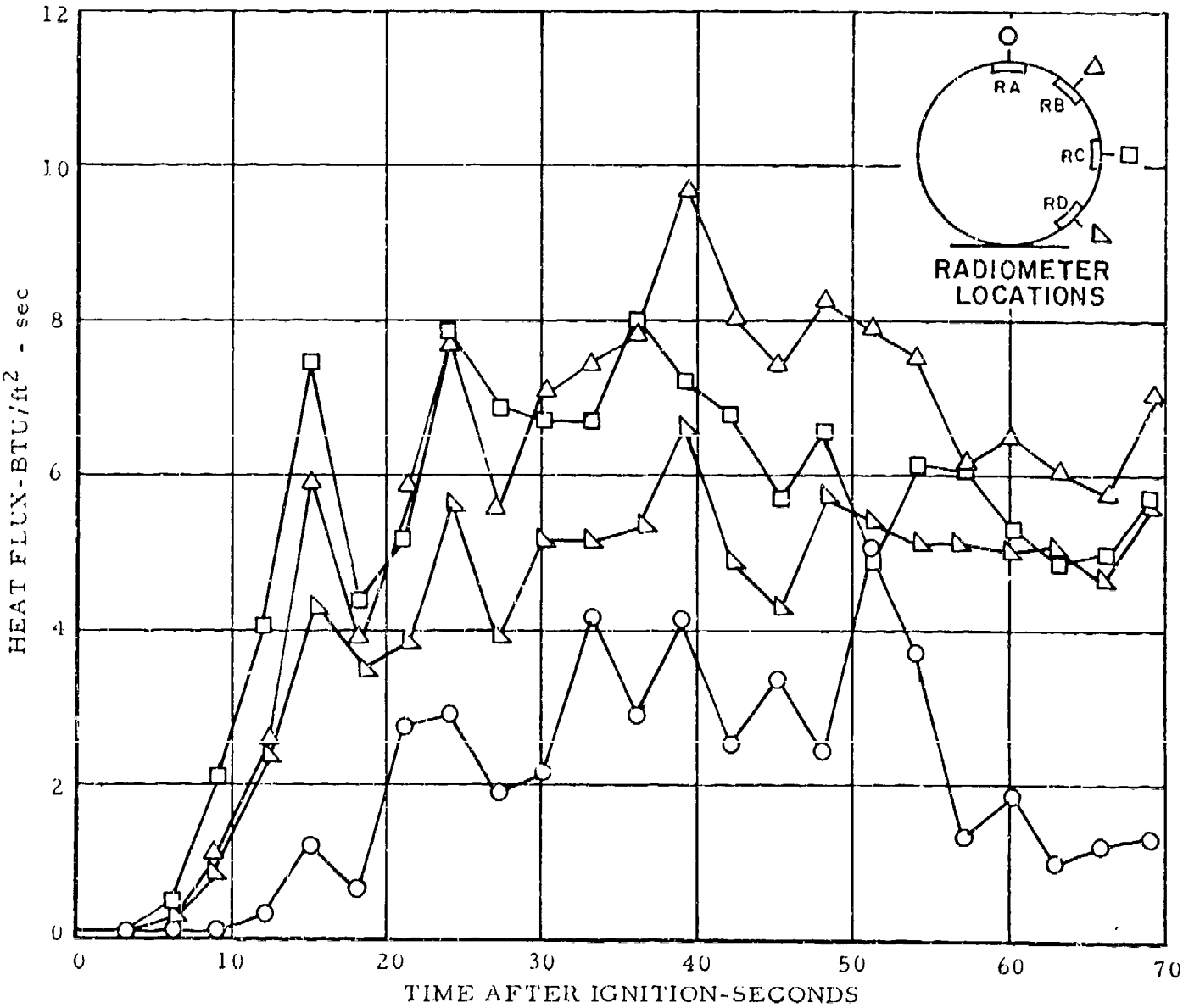

FIG. 3.3 TEST NO. 7 - RADIOMETER DATA FOR ALUMINUM ALLOY 7075-T6 ALCLAD (0.020-INCH THCKNESS)

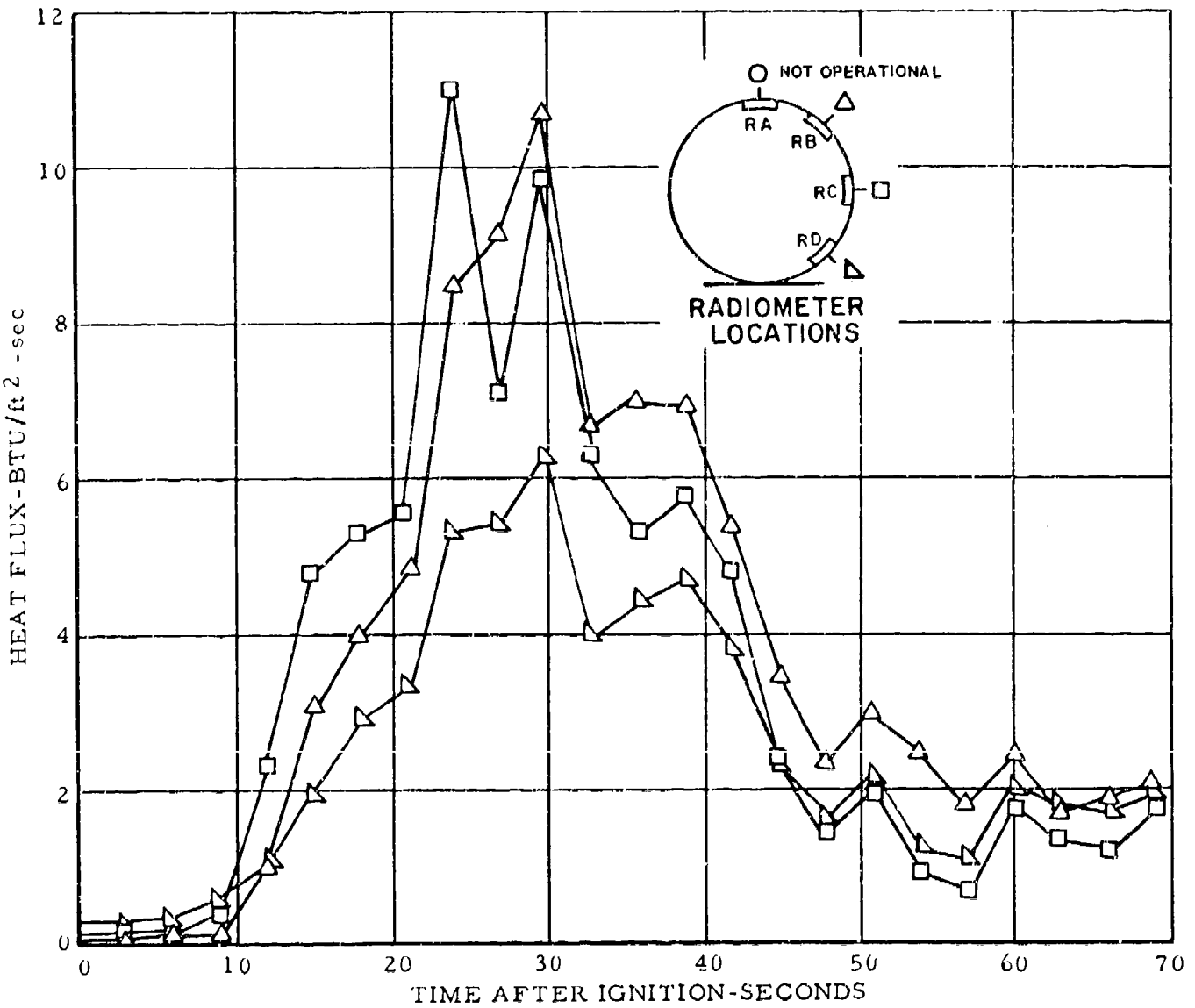

FIG. 3.4 TEST NO. 8 - RADIOMETER DATA FOR ALUMINUM ALLOY 7075-T6 ALCLAD (0.090-INCH THICKNESS)

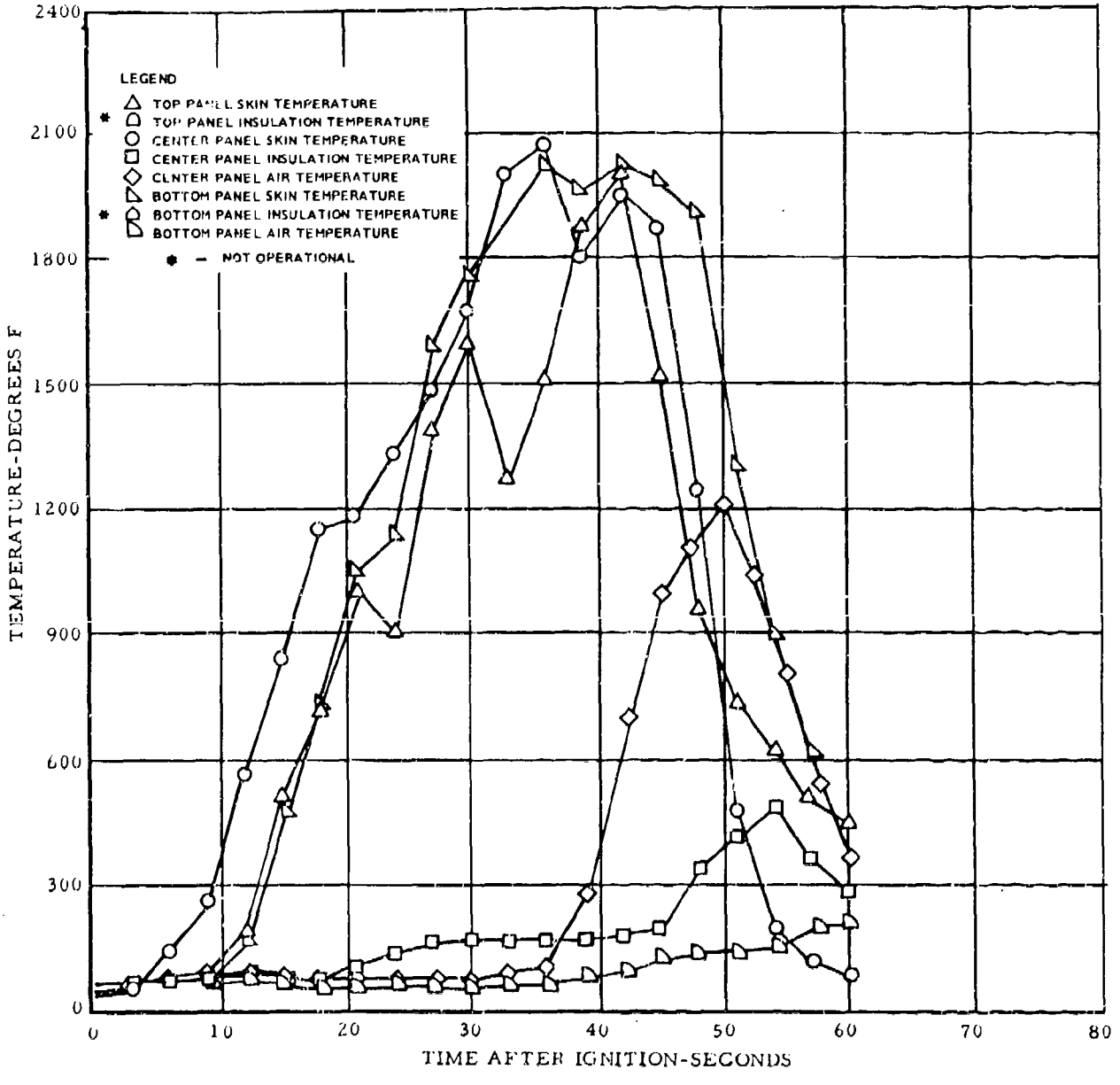

FIG. 3.5 TEST NO. 5 - THERMOCOUPLE DATA FOR ALUMINUM ALLOY 2024-T3 ALCLAD (0.016-INCH THICKNESS)

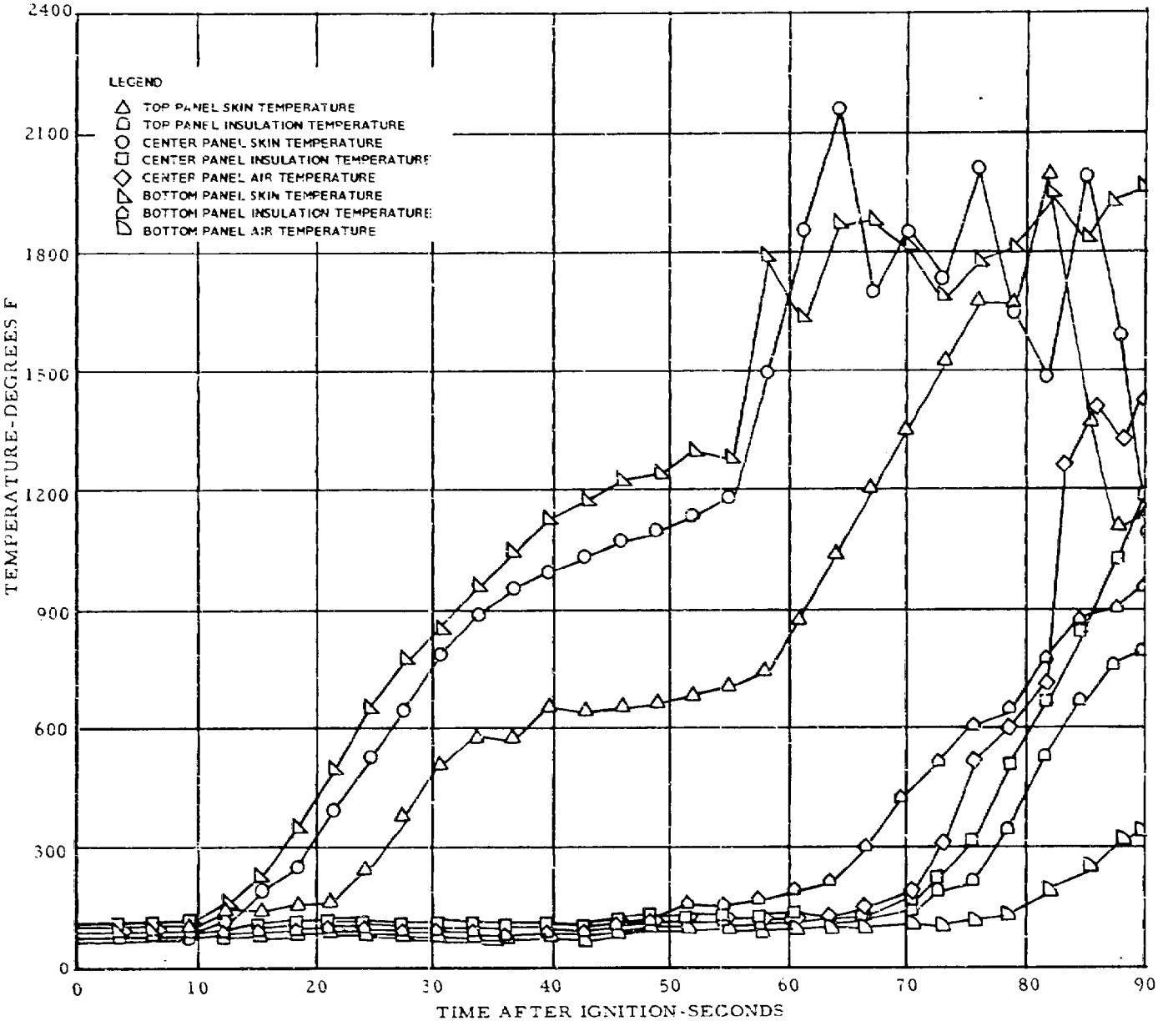

FIG. 3.6 TEST NO. 6 - THERMOCOUPLE DATA FOR ALUMINUM ALLOY 2024-T3 ALCLAD (0.040-INCH THICKNESS)

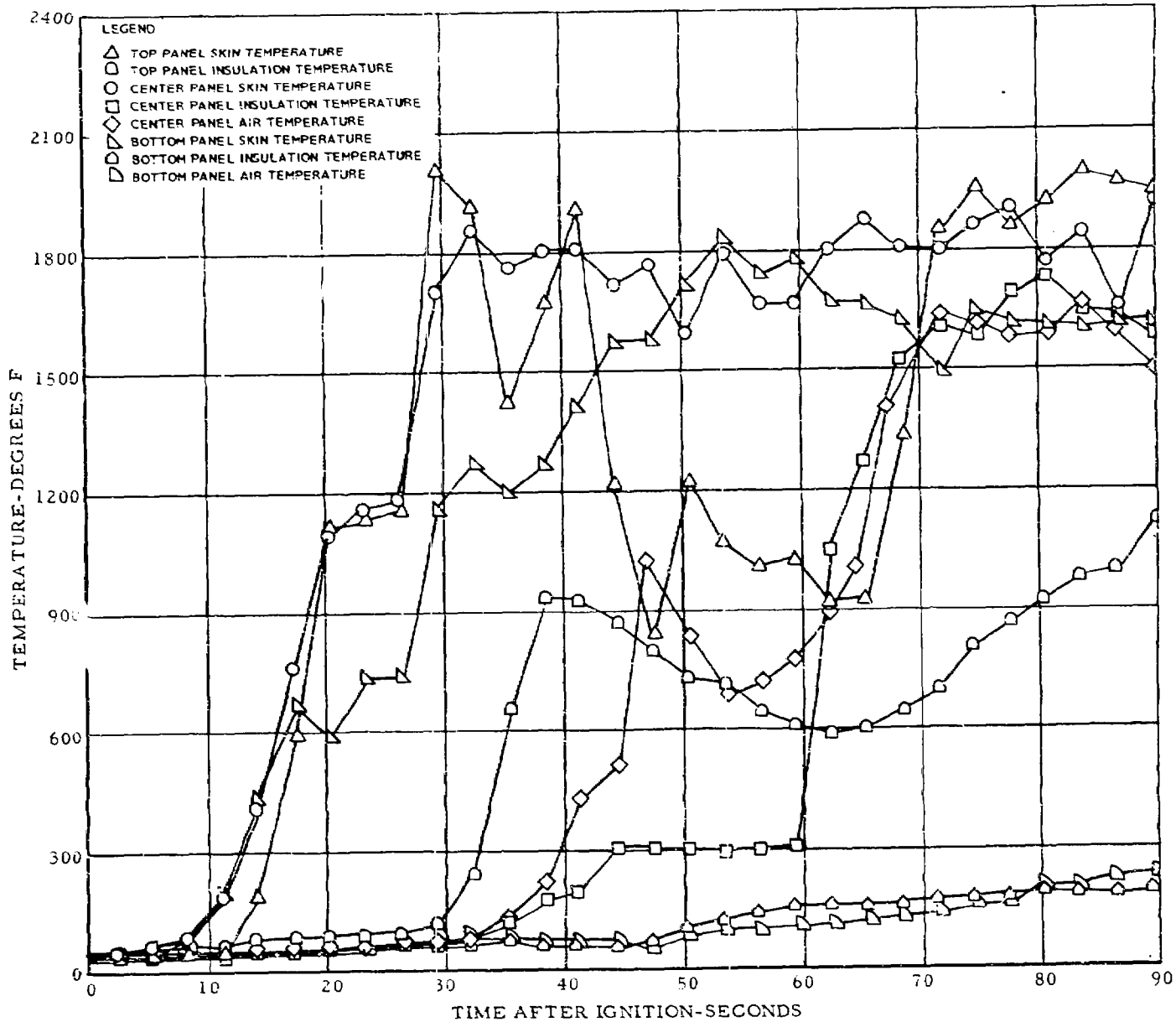

FIG. 3.7 TEST NO. 7 - THERMOCOUPLE DATA FOR ALUMINUM ALLOY 7075-T6 ALCLAD (0.020-INCH THICKNESS)

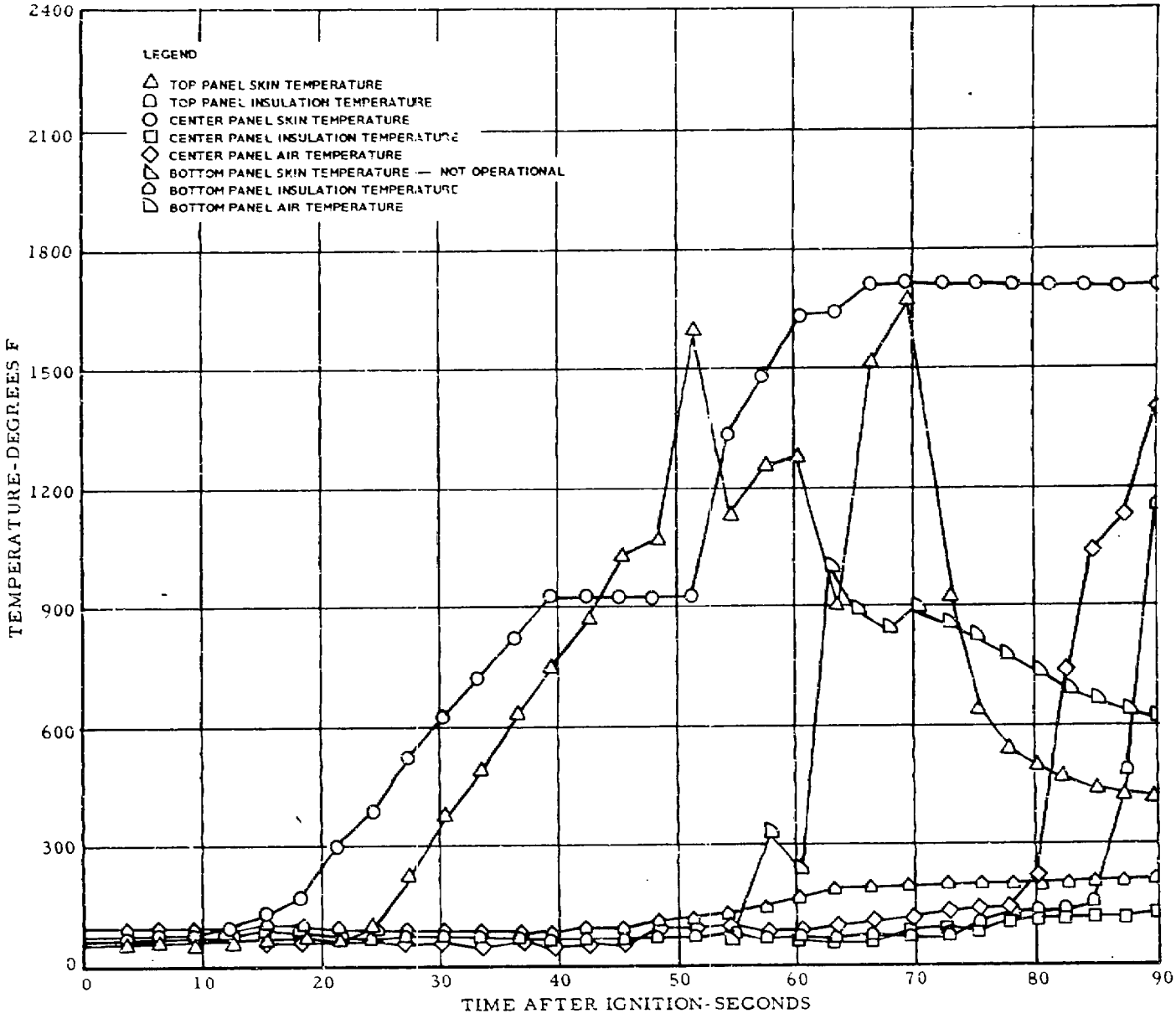

FIG. 3.8 TEST NO. 8 - THERMOCOUPLE DATA FOR ALUMINUM ALLOY 7075-T6 ALCLAD (0.090-INCH THICKNESS)

APPENDIX IV

DEVELOPMENT OF THE MATHEMATICAL MODEL

DEVELOPMENT OF THE MATHEMATICAL MODEL

The development of the mathematical model was based upon heat transfer to and from the aircraft fuselage under conditions where the fire directly contacts the aircraft.

Figure 4.1 shows a simplified model of the aircraft skin backed by a layer of thermal insulation.

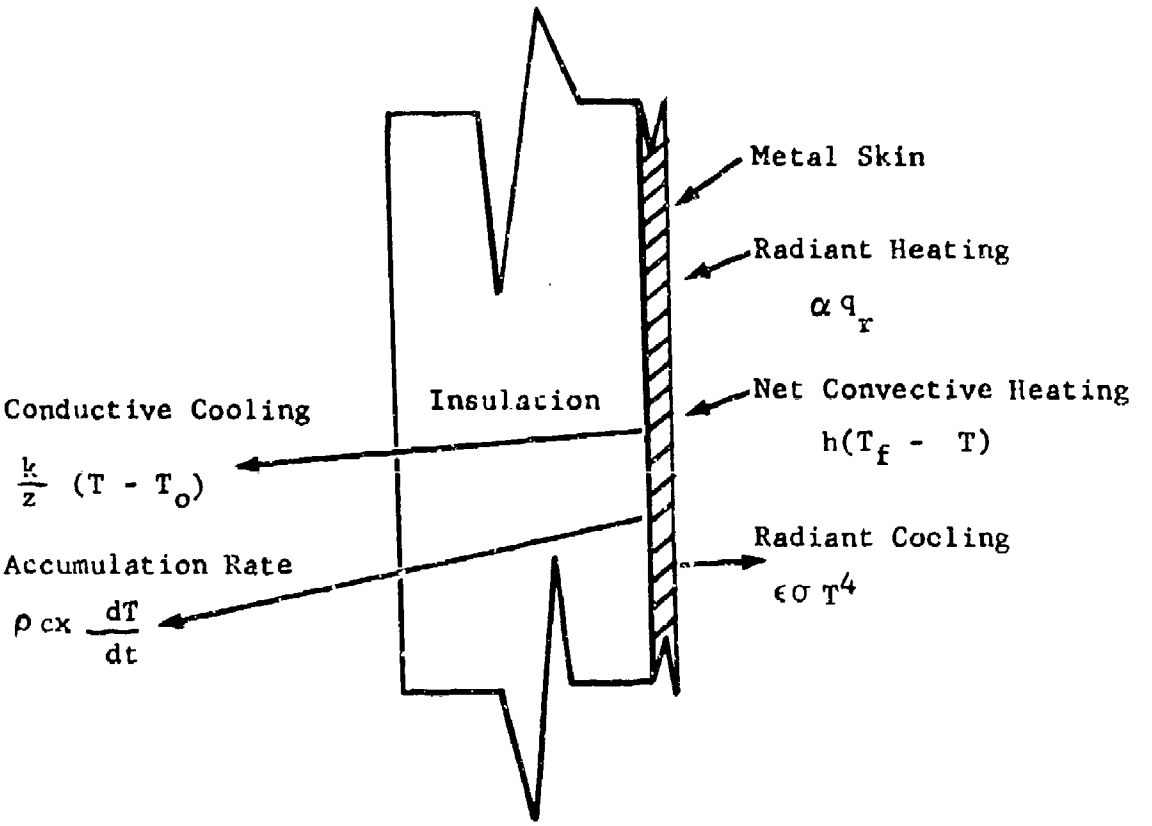

Fig. 4.1 Simplified Model of Aircraft Heating.

In the model, heat gain to the aircraft skin is assumed to be by radiation and convection from the fire. Heat loss from the aircraft skin is due to radiation, convection, and conduction. The difference between the heat gain and heat loss is accumulated by the skin and raises its temperature. The following terms are therefore included in the heat balance.

Radiation heating	$= \alpha q_r$	(1)
Radiation cooling	$= \epsilon \sigma T^4$	(2)
Net convective heating	$= h(T_f - T)$	(3)
Conductive cooling	$= \frac{k}{z}(T - T_o)$	(4)
Accumulation rate	$= \rho c x \frac{dT}{dt}$	(5)

The terms in Equations 1 through 5 are defined as follows:

T = aircraft skin temperature
T_o = temperature inside insulation layer
T_f = flame temperature
α = total absorptance of aircraft skin
q_r = radiant heat output of fire
ϵ = total emittance of aircraft skin
σ = Stephan-Boltzman constant
h = convective heat transfer coefficient
k = thermal conductivity of insulation
z = thickness of insulation
ρ = density of aircraft skin
c = heat capacity of aircraft skin
x = thickness of aircraft skin
t = time

Since

$$\text{Input} - \text{Output} = \text{Accumulation} \qquad (6)$$

Equations 1 through 5 can be combined to obtain

$$\rho c x \frac{dT}{dt} = \alpha q_r + h (T_f - T) - \epsilon \sigma T^4 - \frac{k}{z} (T - T_o) \qquad (7)$$

Equation 7 relates the rate of temperature buildup to the net heat gained by the aircraft skin. In deriving Equation 7, several assumptions have been made in order to simplify the model. The temperature throughout the aircraft skin was assumed to be uniform because the skin is thin and its thermal conductivity is high. The properties of the metal were assumed to be known and constant over the temperature range in question. The radiant heat transfer from the flame to the aircraft was assumed to be constant and the convective heat transfer coefficient was assumed to be constant.

Equation 7 does not account for the amount of energy required to melt the aluminum skin of the aircraft. Since the aluminum is an alloy, it melts over a temperature range rather than at a particular temperature. If it is assumed that the fraction of aluminum melted over a given melting temperature range is proportional to the fraction of the melting temperature range traversed, the heating rate necessary for melting can be given by

$$q_m = \frac{\rho x \quad \Delta H_f}{(T_E - T_B)} \frac{dT}{dt} \qquad (8)$$

In Equation 6

q_m = heating rate for melting

ΔH_f = heat of fusion

T_B = temperature at beginning of melting

T_E = temperature at end of melting

If the energy required for melting is included in the heat transfer equation, it becomes

$$\left[\rho cx + \frac{\rho x \Delta H_f}{(T_E - T_B)}\right]\frac{dT}{dt} = \alpha q_r + h(T_f - T) - \epsilon\sigma T^4 - \frac{k}{z}(T - T_o) \quad (9)$$

Equation 9 can only be used after the initial melting temperature is reached. At temperatures below the initial melting temperature, Equation 7 must be used.

If the skin material does not melt on exposure to fire (for example, a stainless steel skin), Equation 7 can be used throughout the heating cycle and can be used to calculate the maximum temperature reached during fire exposure. The maximum temperature is calculated by setting the accumulation term in Equation 7 equal to zero. Thus,

$$\alpha q_r + h(T_f - T_{max}) - \epsilon\sigma T_{max}^4 - \frac{k}{z}(T_{max} - T_o) = 0 \quad (10)$$

where T_{max} is the highest temperature reached. Equation 10 can be solved by trial and error to obtain the maximum temperature.

SOLUTION OF THE MODEL

Both Equation 7 and Equation 9 must be used for calculation of the failure time for aluminum aircraft skin. Equation 7 applies until the temperature at which melting begins is reached, and Equation 9 applies from the start of melting until melting is complete. Both equations are nonlinear first order differential equations, and neither can be solved analytically. Each requires an initial condition for its solution.

In order to simplify the numerical solution of Equations 7 and 9, they were written in the form

$$\frac{dT}{dt} = A_1 + B_1 T + C_1 T^4 \quad (11)$$

and

$$\frac{dT}{dt} = A_2 + B_2 T + C_2 T^4 \qquad (12)$$

Equation 11 corresponds to Equation 7 and Equation 12 corresponds to Equation 9. The constants are given by

$$A_1 = \frac{\alpha q_r + hT_s + \frac{k}{z} T_o}{\rho c x} \qquad (13)$$

$$B_1 = \frac{(h + k/z)}{\rho c x} \qquad (14)$$

$$C_1 = - \frac{\varepsilon \sigma}{\rho c x} \qquad (15)$$

$$A_2 = \frac{\alpha q_r + hT_s + \frac{k}{z} T_o}{\rho c x + \frac{\rho x \Delta H_f}{(T_E - T_B)}} \qquad (16)$$

$$B_2 = - \frac{(h + k/z)}{\rho c x + \frac{\rho x \Delta H_f}{(T_E - T_B)}} \qquad (17)$$

and

$$C_2 = - \frac{\varepsilon \sigma}{\rho c x + \frac{\rho x \Delta H_f}{(T_E - T_B)}} \qquad (18)$$

The initial condition applied to Equation 11 is

$$T = T_o \text{ @ } t = 0 \qquad (19)$$

since the aluminum is initially at the temperature of the surroundings. The initial temperature for Equation 12 is taken as the initial melting temperature at the time, t, at which the initial melting temperature is reached according to the calculations of Equation 11. Since Equation 12

only applies during the melting period, calculations are stopped when the end of the melting range is reached.

If the aircraft skin is nonmelting material such as stainless steel, only Equation 11 is used, and the calculations are continued until the steady-state solution is approached.

The solutions to Equations 11 and 12 were obtained using the Range-Kutta technique, which is explained in standard books; for example, Mickley, Sherwood, and Reed (Reference 2).

Calculations were made for stainless steel and aluminum aircraft skins using the data in Table 1-IV.

Some of the parameters in Table 1-IV are not well known and must be estimated in order for the equations to be solved. The primary mechanisms for heat transfer within the flame are radiation and convection. Heat transfer by radiation depends not only on the intensity of the source but also on the absorptance of the receiver. The radiant output of the fire, q_r, was assumed to be equal to 31,000 Btu/hr-ft^2, a value obtained by Copley in fire tests using JP-4 as the fuel (Reference 3). Since soot deposits rapidly darken the aircraft skin, the absorptance, α, was assumed to be unity. Likewise, the emittance, ϵ, for the surface was assumed to be unity. The convective heat transfer coefficient, h, was estimated to be 5 Btu/hr-ft^2. The estimate was based on forced convection at gas velocities of about 20 ft/s, and corresponds quite closely to recent data obtained by Neill in direct flame contact heat transfer measurements (Reference 4). The flame temperature, T_f, was taken to be about 2000^{o}F, a value based on optical pyrometer readings on hydrocarbon flames.

It should be pointed out that any parameter dependent on flame properties is not constant. Fluctuations occur which have periods ranging from a fraction of a second to at least several seconds, depending on the turbulance of the flame and the gross movement of the flame due to the effects of external factors such as the wind. However, when the thermal sink is large enough, the small-scale fluctuations, such as those due to turbulance, are damped out.

TABLE 1-IV

NUMERICAL VALUES USED IN CALCULATIONS OF ALUMINUM MELTING TIME

Parameters	ALUMINUM Value	Ref	STAINLESS STEEL Value	Ref
q_r	31,000 $\frac{Btu}{hr\text{-}ft^2}$	3	31,000 $\frac{Btu}{hr\text{-}ft^2}$	3
k	0.7 $\frac{Btu}{hr\text{-}ft^2}$ - $^oF/in$		0.7 $\frac{Btu}{hr\text{-}ft^2}$ - $^oF/in$	
z	0.5 inches		0.5 inches	
ρ	175 lb/ft^3		508 lb/ft^3	
c	0.23 Btu/lb-^oF	5	0.12 Btu/lb-^oF	
ΔH_f	170 Btu/lb	6	NA	
T_B	900^oF		NA	
T_E	1200^oF		NA	
h	5 $\frac{Btu}{hr\text{-}ft^2}$	*	5 $\frac{Btu}{hr\text{-}ft^2}$	*
T_o	80^oF	*	80^oF	*
T_f	2000^oF	*	2000^oF	*
α	1.0	*	1.0	*
ϵ	1.0	*	1.0	*

* See discussion in text of report.